simply positive

D4.1 Geospatial map and report on geo-referenced multi-layer mapping of the PV potential on the example of Focus District of Amsterdam

September 2024

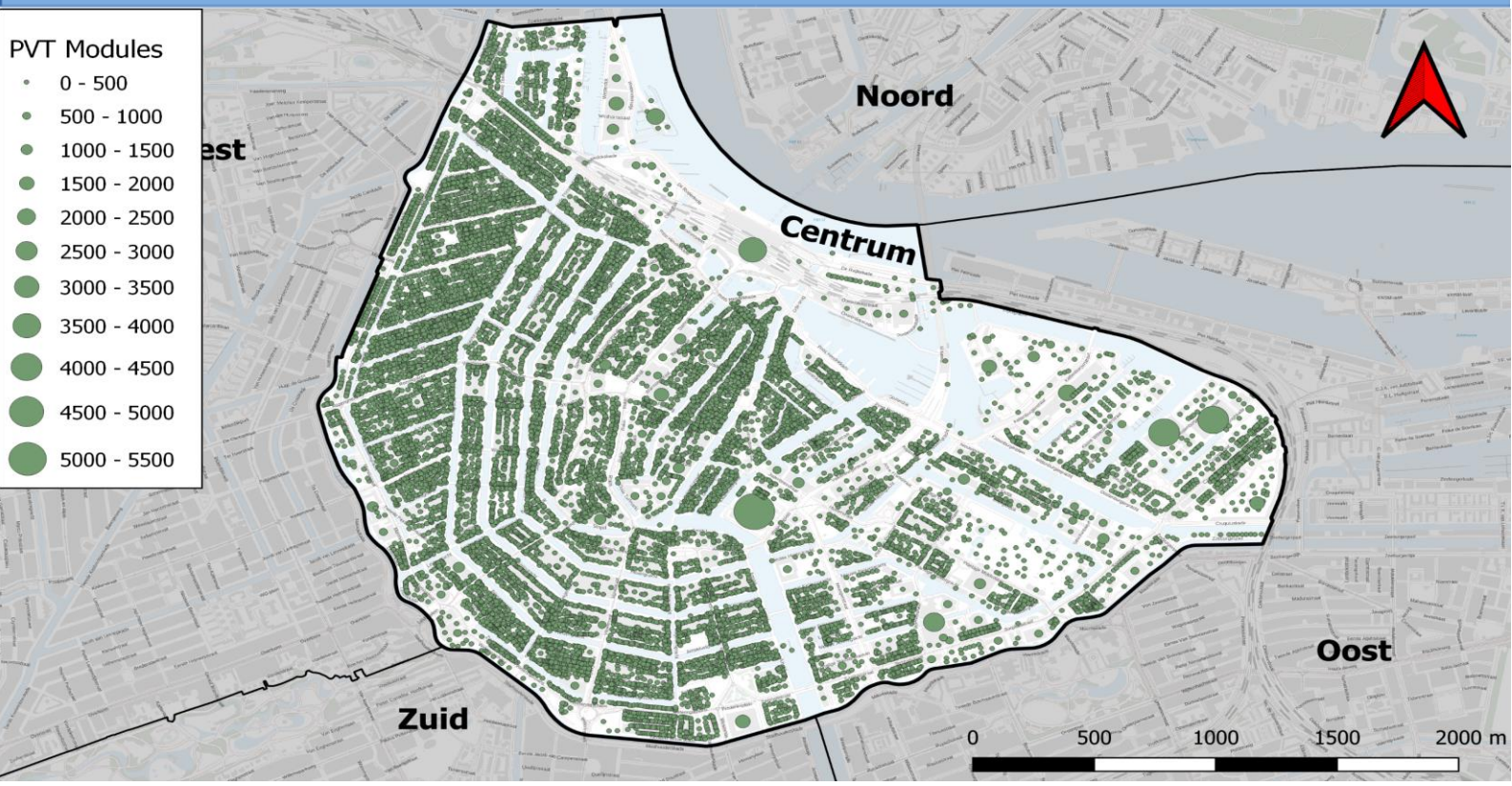

SONNENPLATZ Großschönau

Città di Settimo Torinese

AMS Amsterdam Institute for Advanced Metropolitan Solutions

TU Delft

PV Works

denkstatt create sustainable value

FH University of Applied Sciences Technikum Wien

Reșița

Leader: TU Delft

Dissemination Level

PU	Public	X
CO	Confidential	

History

Version	Description	Lead author	Date
V1	First Template	TUD	Sep 2023
V2	Draft report	TUD	Sep 2024
V3	Review	PVW, AMS	Sep 2024

Disclaimer

This project has been developed in the framework of the PED Program, which is implemented by the Joint Programming Initiative Urban Europe and SET Plan Action 3.2. The Austrian part is supported by the Austrian Ministry of Climate Action, Environment, Energy, Mobility, Innovation, and Technology (BMK); the Romanian part is supported by a grant of the Ministry of Research, Innovation and Digitization CNCS/CCCDI – UEFISCDI, project number PED-JPI-SIMPLY POSITIVE, contracts number 325/2022 and 326/2022, within PNCDI III; the Dutch part is supported by the RVO (the Netherlands Enterprise Agency), reference number ERANETPED-02767306; and the Italian part is supported by a grant of the Ministry of Education and Merit - Department for Higher Education and Research, project number PED_00042, from the Fund for Investment in Scientific and Technological Research (FIRST/FAR) and/or Special Accounting Account no. 5944.

Executive Summary

A geo-referenced multi-layer mapping is realized based on the focus district of Amsterdam, overlaying the PV potential on every roof on other maps, such as roof uses, protected areas, water management, and voltage grid fluctuations. Intersecting information from this complex and informative map, a very realistic PV potential for the whole city and applicability to the other focus districts is carried out. Further on, automation of the decision across different installation modes of PV modules is defined to optimize energy usage and minimize esthetical interference: (a) landscape vs. portrait vs. east-west orientation, (ii) aesthetic compactness of installed PV systems, and (iii) modules visibility from street view. The report also discusses the integration of PVT systems in detail within the urban landscape, ensuring efficient energy generation.

List of Figures

List of Tables

List of Abbreviations and Acronyms

APE	Avoided Primary Energy
BAG	NL: Basisregistratie Adressen en Gebouwen
DHW	Domestic Hot Water
HVAC	Heating, Ventilation, and Air-Conditioning
HP	Heat Pump
LiDAR	Light Detection and Ranging
LCOE	Levelized Cost of Electricity
PV	Photovoltaic
PVT	Photovoltaic-thermal
SCF	Sun Coverage Factor
SH	Space Heating
STC	Standard Test Conditions
ST	Solar Thermal
SVF	Sky View Factor

Table of Contents

1. Introduction

1.1. Purpose of the document

This document aims to provide a comprehensive analysis of the photovoltaic (PV) potential in the focus district of Amsterdam. By employing advanced geospatial mapping techniques and multi-layered data integration, the report identifies optimal locations for solar energy installations. Additionally, the potential of combining rooftop solar thermal (ST) and photovoltaic-thermal (PVT) modules is calculated and compared with the city's future targets. This detailed assessment will help in urban planning and sustainable energy initiatives, supporting the urban district's transition to renewable energy sources.

1.2. Relation to other project activities

In previous years, a study was carried out to estimate the rooftop PV potential energy yield in Amsterdam with the PVW and AMS institute. The project led to the realistic quantification of solar PV potential on Amsterdam rooftops and a comparison with the status of PV installations. In the developed modeling framework, height data of the terrain is used to digitally build the urban fabric, recognize rooftops with respect to cadastre data, automatically place PV modules on rooftops, and accurately compute the PV systems yield up to the AC-side for every building. All this is accomplished with a pace of 2.4 buildings/second. These numbers are already used by the municipality of Amsterdam, which is supporting the Simply Positive project, to engage citizens and plan in time PV installations with accelerated permit certifications.

1.3. Structure of the document

The remaining document is structured to comprehensively address the various aspects of evaluating and implementing PV systems. Section 2 presents geo-referenced multi-layer mapping, providing a spatial analysis framework crucial for identifying optimal PV installation sites. Section 3 discusses methodology for deriving realistic PV potential, incorporating factors such as climate conditions and applicability to other focus districts. This is followed by installation modes and aesthetic considerations, balancing technical feasibility with visual and architectural integration. Moreover, the energetic output of PV(T) modules integrated with Heat pump and seasonal storage is presented in section 5, showcasing their electrical and thermal yields. The document concludes with the findings, highlighting key insights and recommendations.

2. Geo-referenced multi-layer mapping

2.1. Focus district of Amsterdam

Amsterdam, known as the capital city of the Netherlands, has a population of 921,402 within its urban area. The city is taking initiative to harness solar energy through innovative urban strategies, as illustrated in Figure 1, showing an aerial view showcasing Amsterdam's city center buildings equipped with solar panels. At the forefront of this effort is a comprehensive geo-referenced multi-layer mapping and this involves overlaying detailed data on the potential for PV installations onto existing maps that includes roof uses, protected areas, water management systems, and voltage grid fluctuations. By integrating these layers, the aim is to provide a realistic assessment of the city's overall PV potential, while also assessing its applicability to other urban districts.

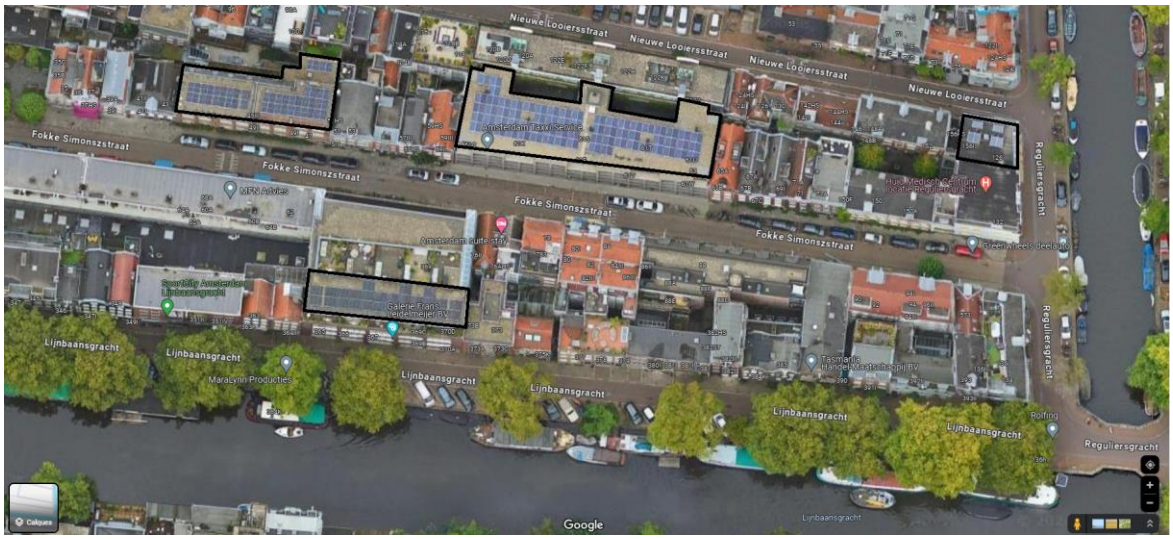

Figure 1: Aerial view showcasing Amsterdam's city center buildings equipped with solar panels.

The complexity of the mapping process extends beyond identification of suitable rooftops; it involves an advanced analysis aimed at optimizing both energy efficiency and aesthetic integration. Automation plays a key role, defining various distinct installation modes for PV modules. These modes include considerations such as orientation, aesthetic compactness of installations and visibility from street view. Furthermore, it also considers the energetic output of PVT modules combined with heat pump and a seasonal storage. Such planning not only ensures maximum utilization of solar resources but also minimizes the visual impact on Amsterdam's urban area, thus fostering sustainable development practices that can serve as a model for urban districts worldwide.

2.2. Overlaying PV potential on Roof Maps

The integration of solar systems into urban environments requires careful analysis of several factors influencing their potential and efficiency. This section provides an examination of

overlaying PV potential (illustrated in Figure 2), focusing on the maximum possible installed capacity and the impact of concurrent roof purposes in the focus district of Amsterdam.

2.2.1. Maximum possible installed capacity

To determine the maximum possible installed capacity of PV systems on the roofs within the focus district involves an extensive analysis of several geospatial elements. By utilizing advanced geo-referenced multi-layer mapping, the available roof space suitable for PV installations can be identified and quantified.

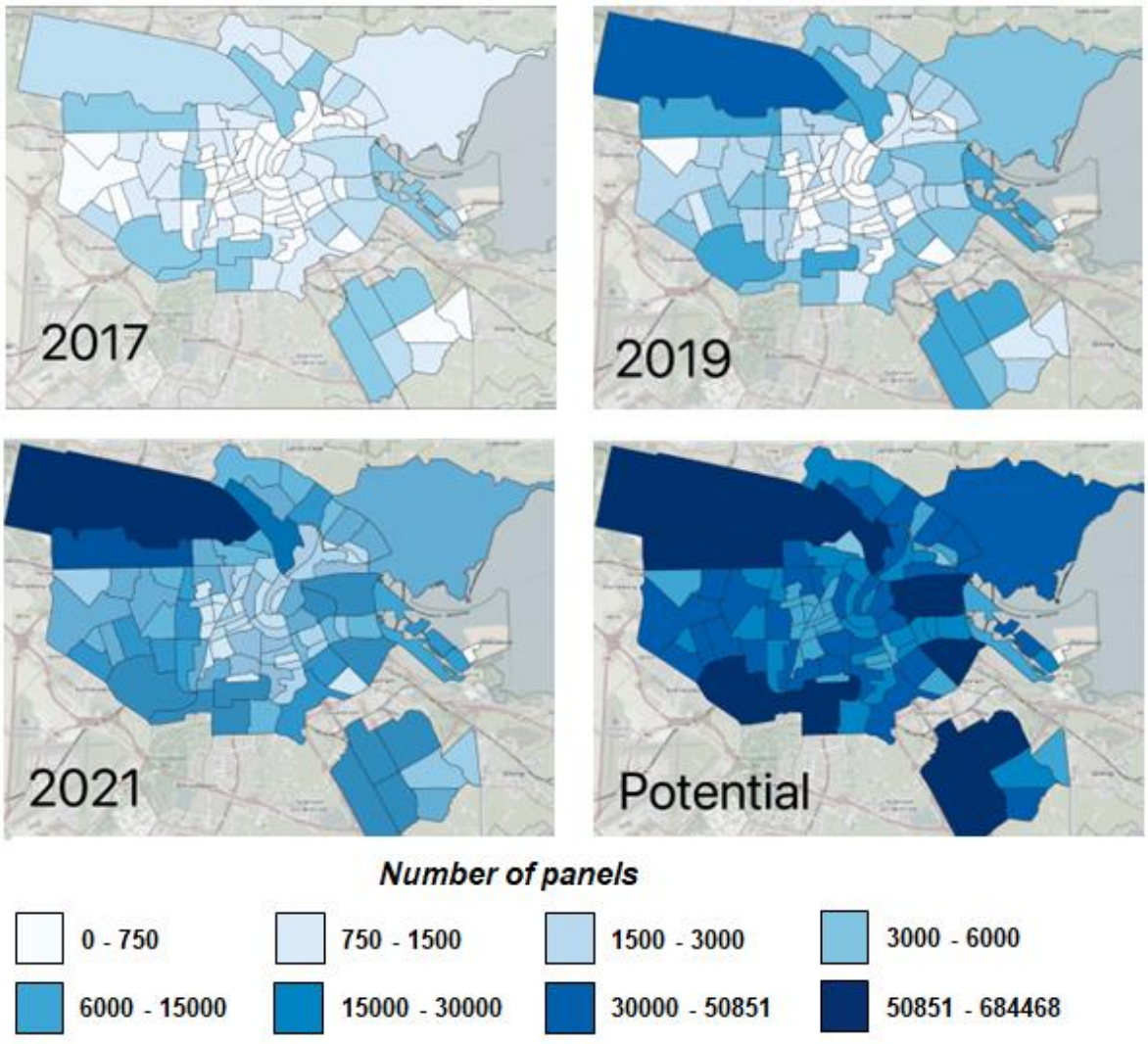

Figure 2 - Progress of installed PV per district and potential in Amsterdam city.

Suitability analysis

- Each roof segment is analyzed for its suitability for PV installation, considering factors such as roof material, structural strength, and solar irradiation [1].
- Roof areas with substantial shading or those structures that are weak to handle additional weight are excluded from the potential capacity calculation.

Roof area calculation

- Using LiDAR data and high-resolution satellite imagery, the roof areas of all buildings within the focus district are defined.
- The surfaces of the roof are categorized based on their tilt, roof orientation and shading effects from nearby buildings or vegetation [1].

Scenario analysis

- Different scenarios are assessed, including different orientations that are landscape, portrait, and east-west to identify the optimal arrangement for maximizing capacity and energy yield.
- The impact of integrating advanced PV technologies, such as PVT modules, is also examined to improve the overall potential.

Energy yield estimation

- To estimate the maximum possible installed capacity of solar collectors, suitable roof areas are then used. This is obtained by utilizing standard PV, ST, and PVT modules dimensions (approximately 2 m^2 module) and parameters.
- The potential energy yield is estimated based on local climate data, standard module efficiency and considering a few assumptions that are indeed part of the module's simplifications. However, it is essential to emphasize that these assumptions are considered minor in the context of the overall thermal model.

2.2.2. Reduction in potential due to concurrent roof purposes

The maximum installed capacity indicates the highest energy a solar collector can generate. However, actual PV potential may be limited by concurrent roof uses, such as existing infrastructure, usage restrictions, communication equipment, roof gardens, and regulatory constraints as presented in Figure 3.

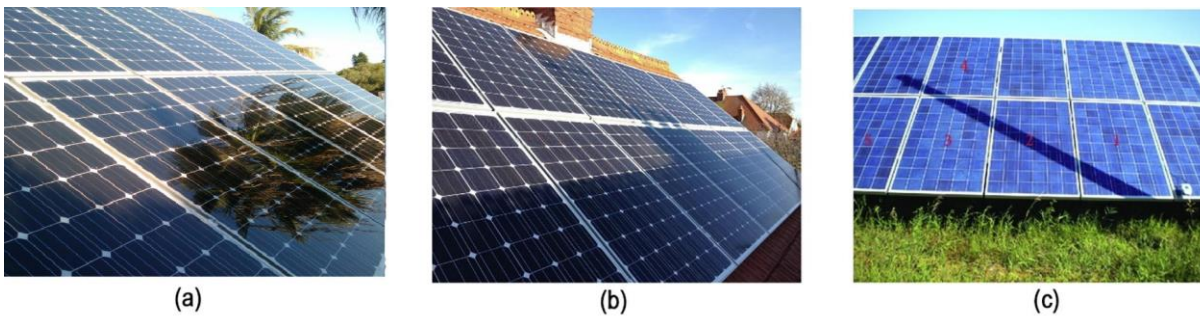

Figure 3 - Shading effect on the solar PV array by concurrent roof uses (a) vegetation, (b) existing infrastructure, (c) communication equipment.

Identification of concurrent roof usage

- Roofs may be used for various concurrent purposes, including heating, ventilation, and air-conditioning (HVAC) installations, water storage tanks, structural elements, and vegetation.
- To understand the spatial distribution and impact on available roof space for solar installations, detailed mapping and classification is carried out.

Impact on solar potential

- Each identified roof use is evaluated for its impact on the space and potential solar installation areas.
- For example, storage tanks and HVAC units occupy significant roof space and can cast shadows on the modules, reducing to capture sun light and the effective area for solar installations and thus decreasing their energy yield.
- Roof gardens may have usage restrictions that limit the installation of the modules and add weight to the roof. Additionally, antennas, satellite dishes can cast shadows and interfere with module placement.

Realistic potential

- The roof areas affected by concurrent use are eliminated.
- After carefully considering all concurrent roof purposes, the realistic potential for solar collectors is obtained.

Building specific limitations

- Historic buildings are identified, their preservation guidelines are considered.
- Protected areas or buildings with heritage status may have strict rules and restrict changes to the roofs, further reducing the potential capacity.

A realistic estimation of the solar modules yield is obtained by overlaying the PV potential on roof maps and considering concurrent roof purposes in the focus district of Amsterdam. This report not only emphasizes the maximum achievable installed capacity but also offers insights into the challenges and opportunities for optimizing solar installations in urban environments.

2.3. Integration of additional maps

The city of Amsterdam hosts many of the geospatial maps used in addition of the calculated potential. Since the potential is calculated per building, each of which has a unique building identification, the results can be easily filtered using maps that feature buildings. In case the map uses a different geometry, some analysis is needed before the data can be linked to the calculated potential.

Roof uses

The municipality keeps track of roof uses using the map called roof landscape [2]. The use color coding to distinguish between roofs used for nature (green), for water management (blue), energy like solar, wind and heat (yellow) and recreation (red), illustrated in Figure 4.

Per address there is a value of the surface area used for each of these subjects. This can be compared with the detected roof space to see if there is enough room left for PV modules on the building.

Protected areas

There is a map [3] with designated protected cityscape areas in the city. Buildings within these areas have more limited options for the implementation of PV. This means we can use this map and filter all the buildings that are within the boundaries of the polygon. Another map hosted by the municipality indicates which buildings are identified as historic monument [4]. This map can be directly used to filter out buildings from the calculated potential map.

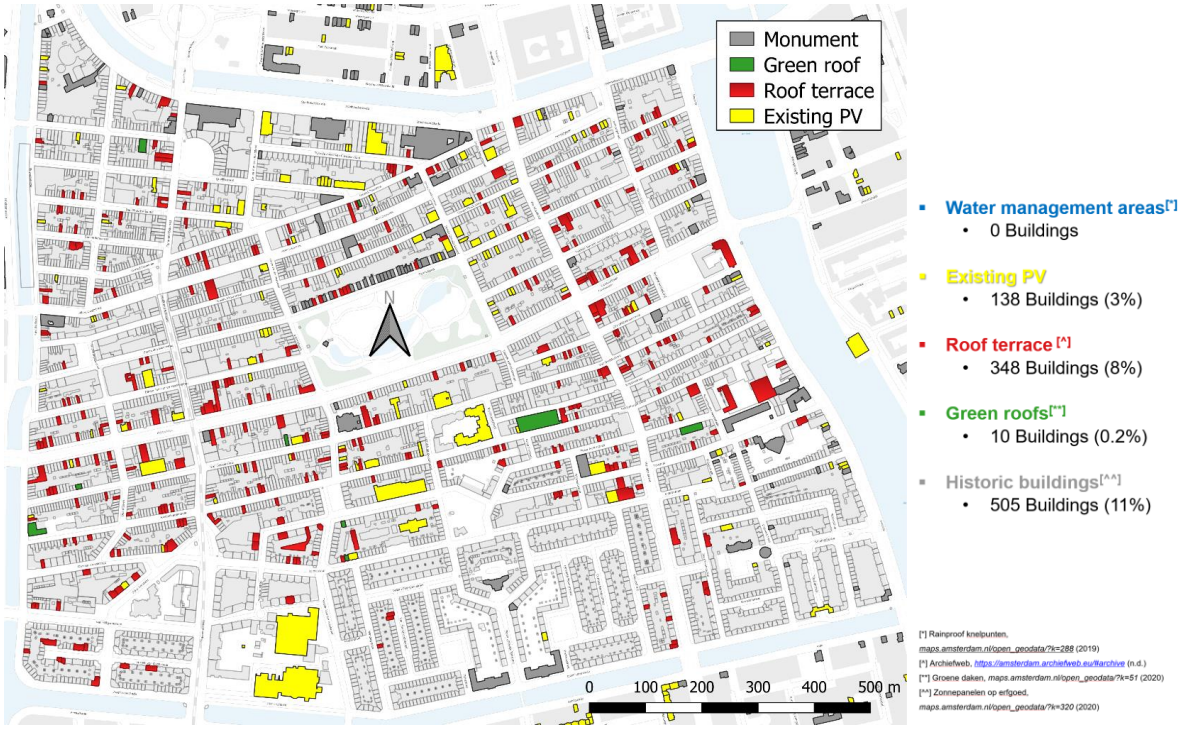

Figure 4 - Multi-layer map for the district in Amsterdam.

Water management

As mentioned in the Roof uses section above, there already is a map with buildings that have used their roofs to help retain water. But another useful map [5] to see which buildings should potentially do the same was shared by a company called rainproof in 2019. This map shows areas that are in urgent, very urgent or extremely urgent need to manage water retainment, to prevent floodings of the streets during heavy rainfall. In this study we filter out buildings that are in extremely urgent areas.

Voltage grid fluctuations

The grid voltage was calculated using a linear power flow grid model [6]. Results of the study case de Pijp can be seen in Figure 5. The redness of the buildings represents the overvoltage per unit (p.u.) compared to the nominal voltage, which is calculated from the nearest medium

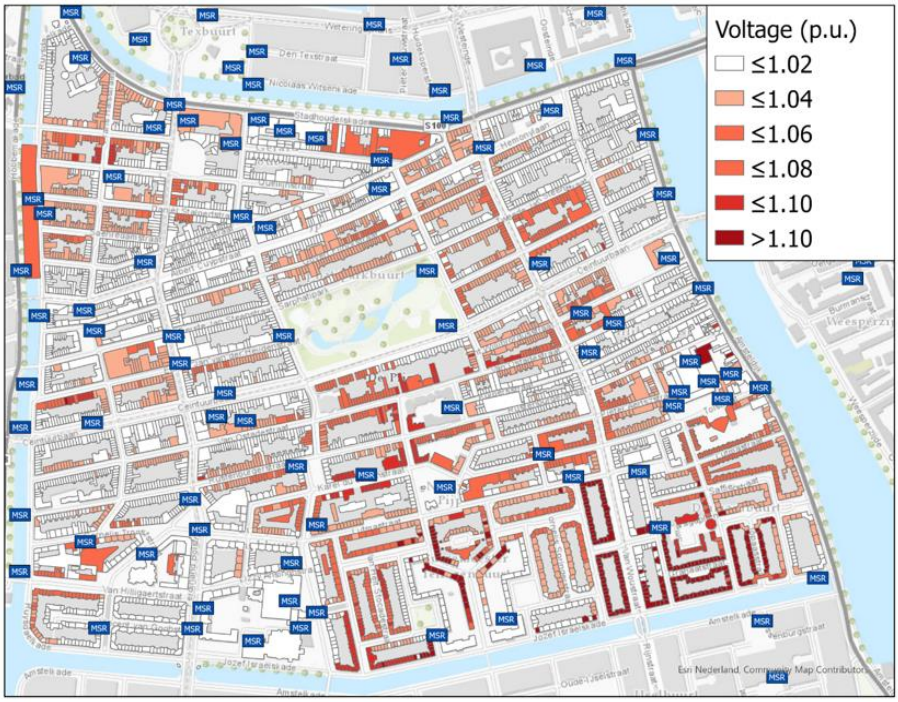

Figure 5 - Voltage disturbance simulation in case of 100% PV penetration at a summer's day at noon.

voltage transformers, indicated with "MSR". Building blocks in the south of this neighborhood surpass the limit of 1.1 p.u. This could lead to an instantaneous shut-down of the MSR, and via a domino-effect to a total black-out. Therefore, these building groups must be filtered out of the potential map to guarantee system security.

3. Deriving realistic PV potential

3.1. City wide PV potential

3.1.1. Input data

In the current approach, LiDAR data serves as the foundation for assessing PV deployment potential. We start with LiDAR point clouds classified as buildings to identify planar surfaces suitable for PV array installation. Our selection criteria benefits non-curved surfaces exceeding 10 m². For flat rooftops, modules are oriented southward with a tilt angle of 13 degrees or east-west with a 10-degree tilt. On sloped rooftops, both portrait and landscape orientations are considered. Furthermore, hourly meteorological data, along with PV module characteristics, inform our analysis to estimate annual PV energy yield. Figure 1 illustrates our modeling framework, which integrates LiDAR data processing with a skyline-based approach to assess PV deployment viability.

LiDAR height data

The new version of the *Algemeen Hoogtebestand Nederland* height data (AHN4) for the years 2020 and 2021 is used and is accessible through the *AHN viewer* [7]. This dataset comprises a Light Detection and Ranging (LiDAR) point cloud with an average resolution of 25 cm, which was processed into a digital surface model with a grid size of 50 cm for analysis. These raster data are organized into tiles measuring 2.5 by 1.25 km, necessitating district-wise processing within Amsterdam.

BAG cadaster building data.

The *Basisregistratie Adressen en Gebouwen* (BAG) data, retrieved from the Cadaster on June 6th, 2023, encompasses 545,288 addresses corresponding to 194,380 buildings citywide. Each building's footprint is defined as a 2D polygon using X and Y coordinates [8].

Climate data

Hourly meteorological data collected from weather stations in and around Amsterdam determine typical weather patterns over an average year. Historical weather data spanning multiple years are utilized to generate a dataset of 8760 hours, incorporating parameters important for computing time-dependent solar irradiance on PV and ST modules.

Table 1 - Parameters of the archetype PV module utilized in this study.

Parameter	**Value**
PV module length (m)	1.669
PV module width (m)	0.996
PV efficiency at STC (%)	19.6
Open circuit voltage (V)	41.08
Number of cells in series	120
Ideality factor (-)	1.2
Temperature coefficient (%/°C)	-0.027
Ground albedo (-)	0.2
Reflective index (-)	0.1
Top emissivity (-)	0.2
Back emissivity (-)	0.89

Module data

Standard rectangular PV modules, along with their dimensions and mounting height, constitute key input parameters for deployment analysis. Additionally, module characteristics such as efficiency under standard test conditions (STC), open circuit voltage, short circuit current, and other relevant factors derived from datasheets contribute to calculating energy yield. Table 1 presents a summary of the parameters for the PV module panel utilized in this study. Water-based ST with glazing while unglazed photovoltaic-thermal (PVT) collectors are used with an area of approximately 2 m^2. Both thermal and electrical efficiencies of the

collectors at zero reduced temperature (function of operating conditions) are provided in the later part of the document.

3.1.2. Skyline-based model

Figure 6 details our modelling framework to evaluate the PV deployment for a particular site. We start with LiDAR data which are readily available in the Netherlands. In this step, we consider only points that are classified as buildings. Using these points, we detect planar surfaces that are large enough to fit a PV array. Non-curved surfaces larger than 10 m^2 are selected for PV module installations.

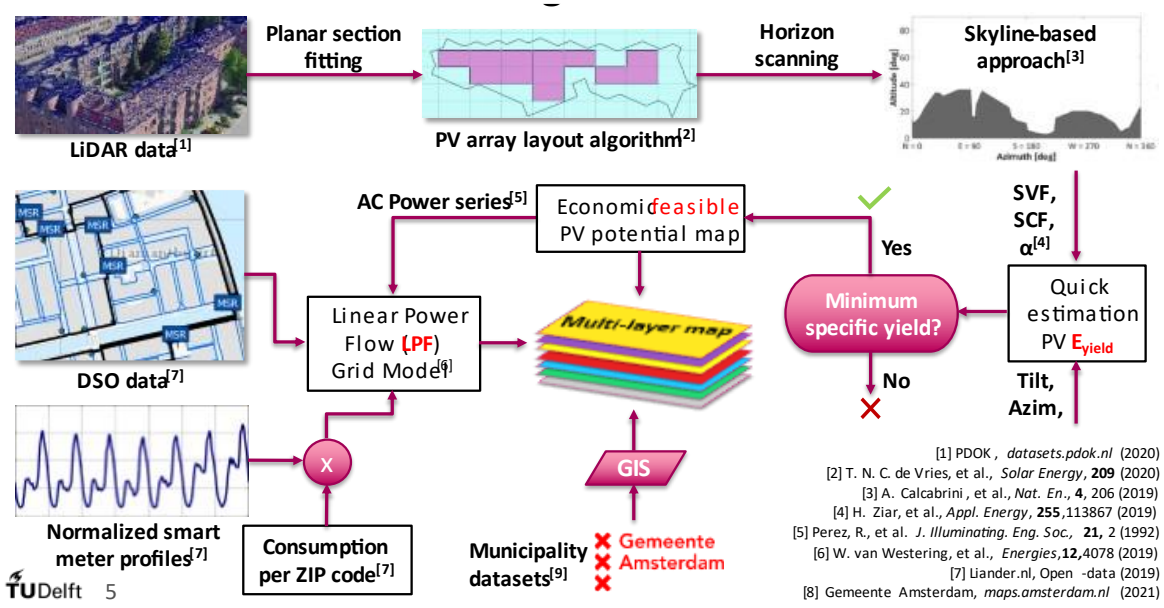

Figure 6 - Modelling framework for the assessment of PV energy yield.

A heuristic layout algorithm is used to fit as many modules as possible in different orientations on the selected surfaces. For flat rooftops, modules are placed facing south with a tilt angle of 13 degrees and a row spacing of 0.7 meter, or east-west with 10 degrees tilt. On sloped rooftops, both the portrait and landscape orientation of modules is assessed.

The surrounding horizon is scanned for each module of the array. In this case we use every Lidar point, including, for example, trees. The horizon scan is used as an input for our skyline-based approach to calculate the energy yield. In this approach we apply the sky-view factor (SVF), sun-coverage factor (SCF), ground albedo, and module tilt and azimuth to make a quick estimation of the annual PV energy yield.

After obtaining the annual PV energy yield per module we check whether the performance of the module is cost-effective. A performance threshold of 650 kWh/kW_p is used to filter out poor performing modules. When the module performance is lower 650 kWh/kW_p the spot is not considered as suitable for PV module installation. Conversely, we consider the spot cost-effective for which we continue to calculate a yearly AC power output. The AC power output

is an input for a linear power flow model, designed to calculate bus-line voltages for grid networks. The result of this model indicates parts of the grid that could lead to voltage problems.

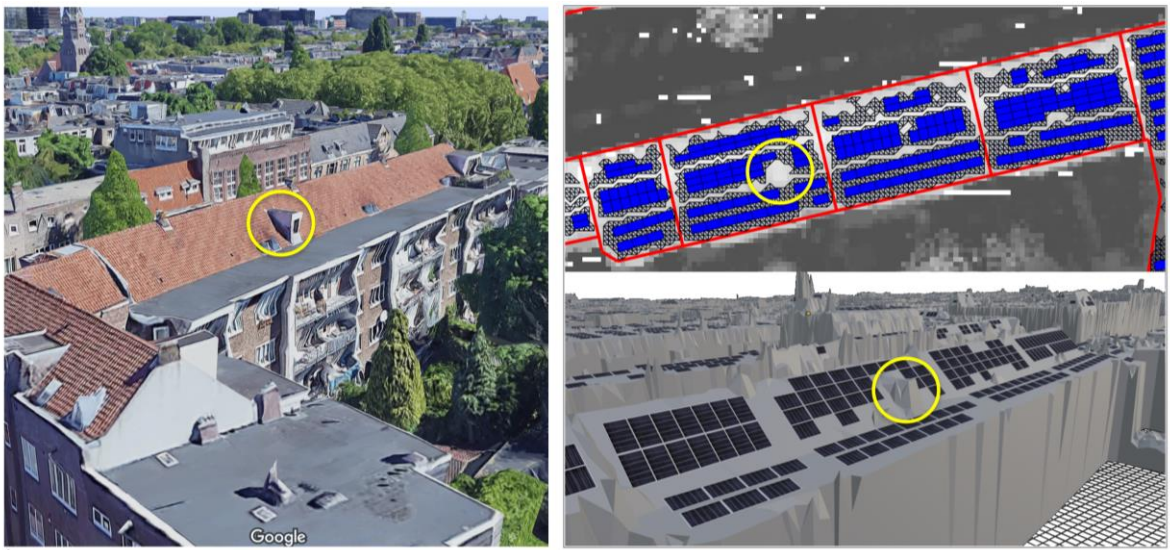

Figure 7 - Detection of available roof space and fitting of PV modules in multiple orientations.

Figure 7 shows how flat surfaces are successfully detected and geometry sticking out-of-plane is ignored. This means that there are gaps in the detected surface where, for example, a dormer was placed at the roof. The horizon scanning approach has been sped up by resampling the height data based on distance. This means nearby points are unchanged, but points far away from the module have been removed at random before doing any further processing. This means a much larger search radius can be used.

3.2. Applicability to other focus districts

This section will be included in a later report due to issues with input data.

4. Installation mode and aesthetic consideration

4.1. Landscape vs portrait vs East-West

A comparison between landscape, portrait, and east-west installation modes for PV modules, with a focus on optimizing energy utilization and minimizing aesthetic impact is investigated in this section. Figure 8b shows that the east-west layout has a higher yield due to the increased number of modules. Although the south-facing orientation depicted in Figure 8a traditionally delivers better performance, its yield may be compromised due to fewer panels. Additionally, the landscape orientation presented in Figure 8d is noted for its efficient panel placement, while portrait orientation illustrated in Figure 8c offers better panel positioning. Through automation, these considerations can be integrated to make informed decisions that balance energy efficiency and visual appeal.

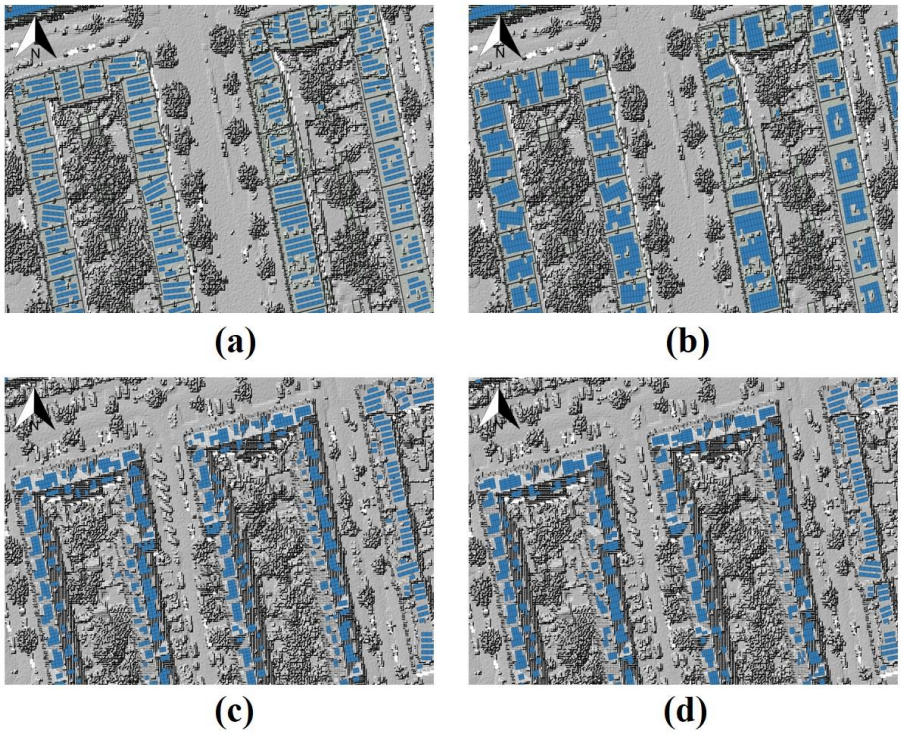

Figure 8 - Layout and orientation for the focus district in Amsterdam: (a) south facing layout for flat surfaces, (b) east-west layout for flat surfaces, (c) portrait orientation for slopped surfaces and (d) landscape orientation for slopped surfaces.

4.2. Compactness of installed PV systems

The compactness of installed PV modules refers to how efficiently the components of the system are arranged within the available space. It is a crucial factor in the design and installation of PV modules as it affects both the aesthetic integration of the system into the environment and the efficiency of energy production. It can be evaluated by comparing the total area occupied by the PV panels with the available surface area.

In PV systems, a more compact arrangement might indicate a more efficient use of space, which can be particularly important in urban environments or areas where space is limited. In assessing the compactness of PV systems, considerations include

- Layout of the panels
- Arrangement of supporting structures
- Integration of the system with existing architectural features

For instance, in a densely built urban area, the PV system should be designed to maximize energy production while minimizing the visual and spatial impact on the surrounding environment. A precise measurement and layout of panels is vital to ensure optimal performance. Poor compactness might result in inefficient energy production or even leave

parts of the system underutilized. Overall, the compactness of installed PV systems is a measure of how well the systems components are optimized in terms of space and efficiency, ensuring that the PV system is both effective and aesthetically integrated into its environment.

4.3. Visibility of modules from street view

In in earlier project of this team, a simulation approach was developed to analyze which PV modules on detected roof space could be visible from public spaces. Guidelines, provided by the municipality, indicated that modules on sloped roofs are allowed as long as they are not visible from public spaces. The approach roughly consists of 4 steps:

1. Identify surrounding pedestrian paths.
2. Place viewpoints on the pedestrian paths.
3. Draw sightlines between the viewpoints and the solar panels.
4. Determine any obstructions to the sightlines.

Pedestrian path search area

A search radius of 75 meters around each building was used to determine if a path should be included in the analysis. We define the direction of a sloped roof surface to be front facing if the closest street is in the direction of the normal of this surface. For rear-facing roof surfaces, according to the guidelines, a distance of more than 20 meters from the public road means it has no street view restrictions.

Viewpoints on pedestrian paths

On each pedestrian path, so-called viewpoints are placed at 10-meter intervals. This chosen value is a balance between calculation speed and accuracy. The street height is determined based on surrounding elevation data plus 1.5 meters to simulate normal eye-level height.

Sightlines to solar modules

Next, a sightline is drawn to the center point of each solar panel, allowing the elevation angle to be determined from the viewer's perspective.

Sightline obstruction

Using the same elevation data as mentioned earlier in this report, data points are search around the sightline. If multiple points are elevated above the sightline, it is likely that the line-of-sight is obstructed. Elevation data on the roof surface close to the panels is ignored to avoid inaccurate placement of the panels being blamed for sightline obstruction. Elevation data outside the contours of buildings is not included, mainly to avoid seasonal variability of vegetation.

5. Photovoltaic-thermal modules energetic output

In PV technology, the solar energy absorbed by a PV module converts into heat, raising the PV cells temperature and reducing its performance and lifespan. The cell efficiency drops by about 0.30 - 0.45% per 1 ^{o}C increase in cell temperature, depending on the cell technology. Cooling can improve the PV efficiency [9]. Integrating a cooling mechanism using air or liquid can enhance PV performance, generating both electricity and thermal energy from the same area.

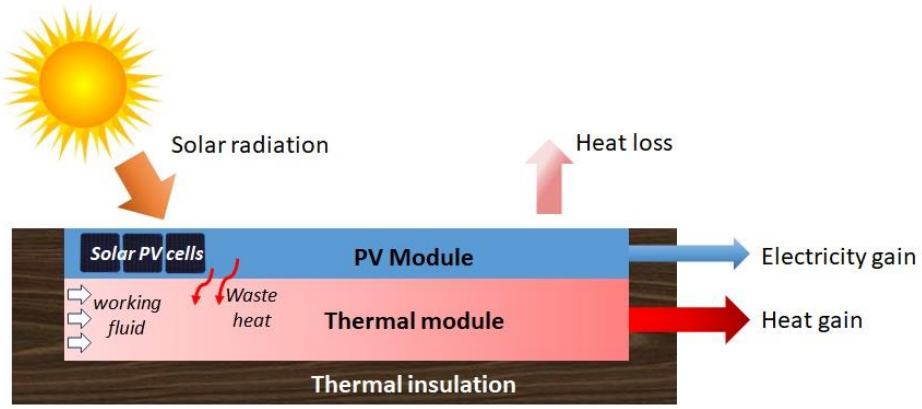

Figure 9 - Schematic diagram of a PVT collector featuring integrated PV and thermal modules for simultaneous electricity generation and heat capture [10].

Photovoltaic-thermal (PVT) collectors, combining PV and solar thermal (ST) modules, are gaining attention for their dual heat and electricity generation capabilities as shown in Figure 9. Researchers focus on liquid PVT systems since the early 2000s due to their benefits over standalone PV or ST modules. Despite being more complex, PVT systems offer higher total efficiency. Water and air are two common heat extraction mediums, water is generally more efficient than air due to its higher thermophysical properties, often mixed with glycol to prevent corrosion and freezing. Air-based collectors avoid freezing and leakage but are less efficient in cold climates. These systems have various potential applications [11], water-based systems are preferred for water heating, cooling, and industrial processes, while air-based systems are better for drying and space heating. These collectors have distinct designs and configurations, unglazed collectors are efficient at electricity generation but less effective for heating. The combined system also reduces the need for separate installations, saving space and potentially lowering overall installation and maintenance costs. Moreover, PVT collectors contribute to a reduced carbon footprint by maximizing energy output from the same surface area, supporting more sustainable and efficient energy production.

5.1. Key performance indicators

Key performance indicators (KPIs) for solar energy systems are important metrics that quantify the effectiveness and efficiency in converting solar energy into usable electrical and thermal energy. The primary KPIs include efficiencies of the collectors, avoided primary energy, COP of the heat pump and thermal efficiency of heat storage.

Electrical efficiency of the module

Electrical efficiency of the PV module calculates the fraction of solar radiation that the PV module converts into electrical energy and directly affects the electrical power. The electrical efficiency of the module depends on the type and material of the cell, its design, and climate conditions such as ambient temperature, solar irradiation, and wind speed. Typically, new available commercial solar PV modules have an electrical efficiency of approximately 22%.

Thermal efficiency of the module

Thermal efficiency of a solar collector evaluates its capability to capture and utilize thermal energy. It indicates how effectively the collector converts solar radiation into useful heat for various applications such as space heating, DHW, drying, etc. [11]. The thermal efficiency of the collector depends on its design, tube configuration, heat extraction medium and an insulation. Usually, for liquid-based glazed ST modules, the thermal efficiency is around 75%, whereas for a PVT collector, it can be up to 60%, as depicted in Figure 10.

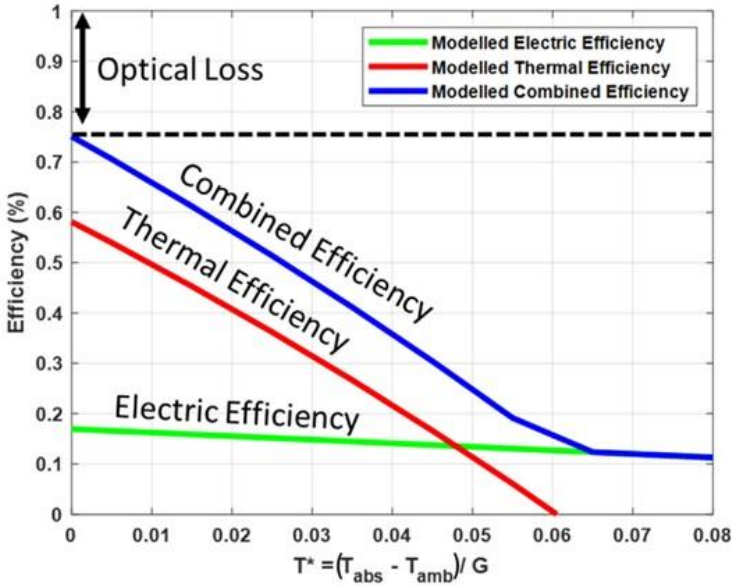

Figure 10 - Performance analysis of a PVT collector: highlighting electric efficiency (green), thermal efficiency (red), and combined efficiency (blue) [12].

Overall efficiency of the PVT collector

The combined efficiency of a PVT collector is calculated using both thermal and electrical efficiencies. It represents the total energy conversion efficiency, accounting for both the electrical and thermal energy outputs relative to the total solar energy incident on the module. The overall efficiency helps in comparing the performance of PVT collector with conventional PV and ST modules. Typically, it varies, depending on type of the collector and its design, for liquid based glazed collectors it can reach up to 80%, whereas in case of air as heat extraction medium and non-glazed collectors, the combined efficiency is lower.

Avoided primary energy of the collector.

One significant KPI is the avoided primary energy (APE) of the collector, which provides a comprehensive measure of the systems effectiveness, accounting for both electrical and thermal energy outputs. It is evident that while the electrical and thermal efficiencies of PVT collectors are individually lower compared to separate PV and ST modules as shown in Figure 11, the total APE per square meter is higher for a PVT collector. This is because of simultaneous production of electricity and heat. The approach involves using the efficiencies of conventional energy conversion methods to determine the weights. Specifically, the APE can be calculated by considering the efficiencies of converting primary energy into electricity (typically 40% for conventional power plants) and heat (typically 65% for conventional gas-fired domestic hot water systems) [10]. This weighted sum approach offers a more accurate representation of the collector's performance.

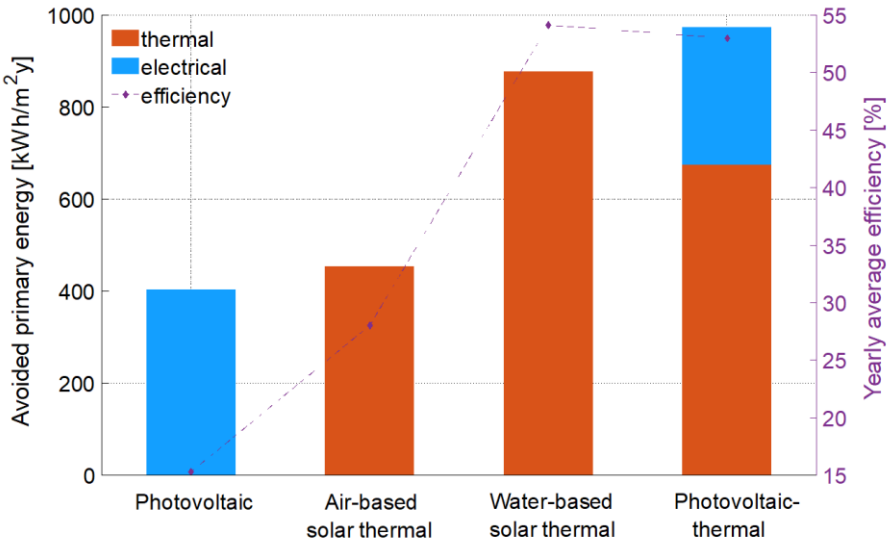

Figure 11 - Average annual efficiency and avoided primary energy comparison of a PVT collector with only PV and solar thermal (both air and water) collectors considering Dutch climate.

Coefficient of performance of heat pump

The COP of a heat pump is a measure of its efficiency and is defined as the ratio of the heat output to the electrical energy consumed. It is an important KPI when assessing the efficiency of the integrated system. A higher COP reduces operational cost and indicates a more efficient heat pump, as it provides more heating or cooling for each unit of electricity consumed. Consider a real case where a residential building with a floor area of 80 m^2 with approximately 2 m^2 of solar collectors installed on the rooftop utilizes this integrated system. The heat pump operates mostly during the winter season when heating is required, the COP typically ranges between 4 and 7 as illustrated in Figure 12.

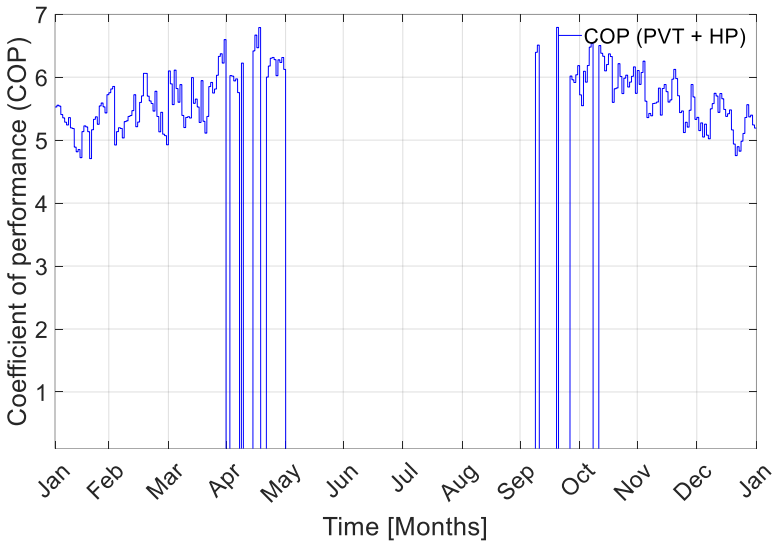

Figure 12 – Annual coefficient of performance (COP) for a building with a floor area of 80 m² and a PVT collector of approximately 2 m².

Thermal efficiency of seasonal storage

The thermal efficiency of seasonal storage is determined by the ability to effectively store and retrieve thermal energy with minimal losses. It is a key metric and is defined as the ratio of energy retrieved to energy injected. It provides a quantitative measure of how effectively the aquifer system retains and returns the thermal energy stored within it, which is crucial for assessing the overall performance of ATES systems.

5.2. Influence of environmental factors and building insulation

The performance of PVT collectors is significantly influenced by various environmental factors, which can affect both their electrical and thermal outputs. Key environmental factors include climate data, weather conditions, building insulation and seasonal variations.

Ambient temperature

Climate data plays a key role in the efficiency of the solar modules and mainly includes ambient temperature, solar irradiation and wind speed. Higher ambient temperatures can lead to high PV cell temperatures which results in lower PV efficiency of the module. Research shows that a PV cell efficiency decreases about 0.30 to 0.45% for an increase of 1 ^{o}C, depending on the specific cell technology employed. However, in case of a PVT collector, the use of heat extraction medium keeps the cell temperature lower, thereby enhancing electrical efficiency of the PV module.

Solar irradiance

Solar irradiation is another factor that directly influences the energy output of the solar modules and is measured in watts per square meter. Both the electrical and thermal energy production increases with the increase in solar irradiation. However, geographic location, season change, and weather conditions can lead to variations in the performance of the solar

modules. The incidence angle at which sunlight hits the solar module affects energy absorption by influencing the amount of solar radiation that is captured and converted into usable energy.

Weather conditions

Weather conditions such as wind speed and cloud coverage also affect the performance of the solar modules. Cloudy conditions reduce solar irradiance, thereby lowering energy output. On the other hand, wind can have a cooling effect on the PV modules, potentially enhancing the PV efficiency but also affecting thermal performance of the thermal modules.

Seasonal variations

The performance of solar modules is influenced by changes in solar incidence, available solar hours, and seasonal variations. Electrical efficiency improves in winter months due to cooler PV cell temperatures, but energy production is lower. Conversely, summer months provides higher irradiance and more solar hours, boosting energy output. The excess heat generated in summer is stored for later use in heating during winter, while the cooler fluid extracted can be used for cooling applications during summer.

Building insulation

Building insulation serves as a barrier to heat loss and is crucial because it directly impacts heating and cooling demands. Well-insulated buildings use less energy, as the heating system needs to exert less effort to maintain the desired temperature, leading to reduced energy costs. In summer, insulation blocks external heat from entering, lowering cooling requirements. Additionally, effective insulation minimizes temperature fluctuations and helps maintain a stable indoor climate.

5.3. Modeling of PVT system components

Modeling approach and description for different components used for the integrated system as illustrated in Figure 13, is briefly described.

5.3.1. Solar thermal module

A simple standard glazed-only ST module is modeled which comprises of components such as a protective glass cover, absorber plate, and an insulating layer to reduce thermal losses while improving structural strength. The additional glass cover minimizes heat losses from convection and radiation, thereby enhancing the thermal efficiency of the collector. The absorber plate, typically made of a highly conductive material, captures solar energy, and transfers it to the circulating fluid within the module. The fluid, which in this case is water, enters from a single point, absorbs heat as it flows through the system, and exits as warm fluid, ready for use in heating. The models exhibit high nonlinearity, introducing significant challenges in the formulation of the ST model. The temperature of each component of the module is assumed to be homogeneous, and horizontal temperature distribution is neglected. Uniform boundary conditions are applied for solar irradiance, wind speed, and ambient temperature. To predict temperatures and evaluate the thermal performance of the module,

the fundamental principle of energy conservation is applied to each component, considering conductive, convective, and radiative thermal exchanges.

5.3.2. Photovoltaic-thermal collector

Different configurations of PVT collectors are modeled. The standard PV module includes components such as a protective glass cover with PV cells embedded in a polymer layer (ethylene vinyl acetate, EVA) and tedlar. One configuration is an air-based unglazed PVT, comprising a standard PV module, an air channel for heat extraction, and an insulator to reduce thermal losses and improve structural strength. The second configuration adds an extra glass cover with an air gap to the air-based unglazed PVT system, minimizing heat losses from convection and radiation, thereby providing more usable energy for heating purposes like space heating and DHW. The third configuration is an unglazed water-based PVT module where water circulates within tubes, entering from a single point and being evenly distributed before warm water is collected at the other end. These models are highly nonlinear, posing significant challenges. For simplicity, a few assumptions have been taken into consideration. Despite these simplifications, the models effectively predict temperatures and evaluate the electrical and thermal performance of the collectors using energy conservation principles, as mentioned above.

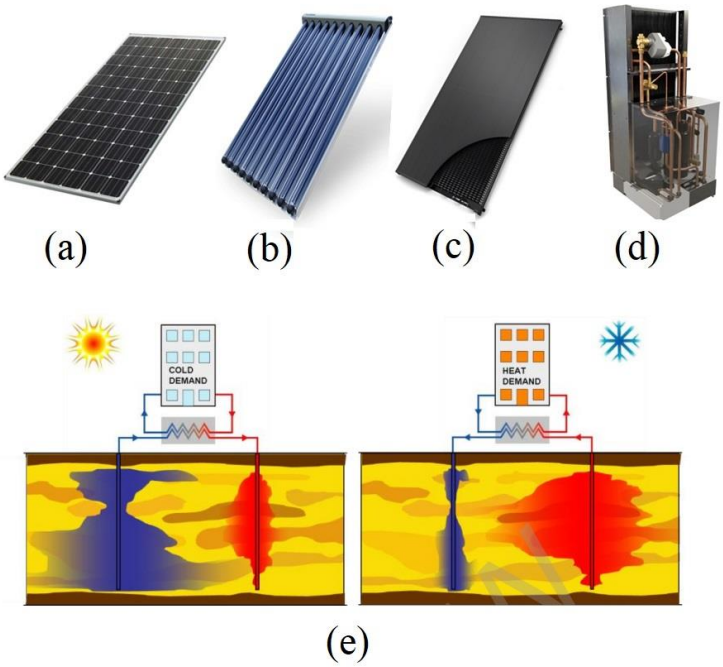

Figure 13 - Main components of the system (a) PV module, (b) solar thermal module, (c) PVT module, (d) water source heat pump and (e) principle operation of an ATES doublet system during summer and winter.

The dynamic models of ST and PVT collectors estimate the temperature distribution of the components of the collector and give a realistic and reasonable annual performance assessment of the collectors. By utilizing real weather data, they accurately predict the systems annual electrical and thermal yield.

5.3.3. Heat pump

A heat pump with the seasonal storage and solar collector plays a crucial role by efficiently transferring heat from one place to another to meet the buildings heating and cooling demands. There are multiple types of heat pumps; however, for this work, a water source heat pump is utilized. To accurately simulate the heat pump, a thermodynamic cycle is used to improve the quantification of the heat transferred for both space heating and DHW demands. The key processes of the heat pump are evaporation, compression, condensation, and expansion. The modeling applied in the thermodynamic cycle is solved for each hour of the year, considering the fluctuating thermal conditions used for both space heating and DHW. During the heating season, water from the warm aquifer (at 25 ^{o}C) or from the ST module is directed to the heat pump, which elevates the temperature to the required levels for space heating (35 ^{o}C) and DHW (60 ^{o}C). Conversely, for cooling, water from the cold aquifer (at 15 ^{o}C) passes through a heat exchanger where it absorbs heat from the building water. The heat pump enhances the systems overall energy efficiency by utilizing the relatively stable temperatures of the aquifers, ensuring that the buildings temperature requirements are met while also managing the thermal balance between the warm and cold aquifers.

5.3.4. Addition of domestic storage tank

Effectively storing the heat generated by solar collectors is crucial. Consider a domestic storage tank and evaluate if it can be effectively utilized with solar collectors to cover the annual demand for heating and electricity. The system integrates a bi-fluid PVT collector that

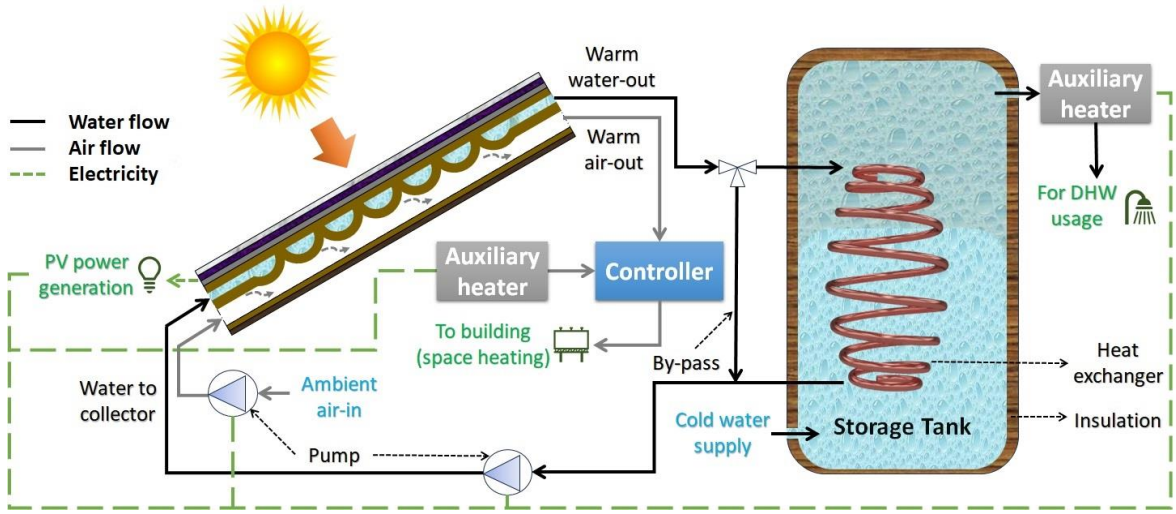

Figure 14 - Schematic diagram of a novel bi-fluid PVT system coupled with a storage tank, auxiliary heaters, and a controller [10].

provides space heating, DHW, and electricity, supported by a domestic storage tank as shown in Figure 14. Solar radiation is available during the day but not during cloudy days or peak winter times. Since heating is mostly needed in the early morning and evening and the storage tank has limited heat retention, auxiliary heaters are essential to maintain a supply of hot water at 60 ^{o}C. Due to the limited capacity of the domestic storage tank, switching to seasonal

storage is necessary to meet the fluctuating demand more effectively, especially during the colder months.

Analysis presented in Figure 15 shows that the heating demand peaks during winter, indicating significant seasonal variation. In contrast, the summer months see a decrease in load, reflecting lower energy requirements for DHW. The system can cover over 30% of the total DHW demand during peak winter months, whereas it can meet between 65% to 80% of the demand for the rest of the year, due to higher solar irradiance levels during the summer. However, to cover 100% of the demand, auxiliary heaters are required, which consume electrical power and are not as efficient as heat pumps.

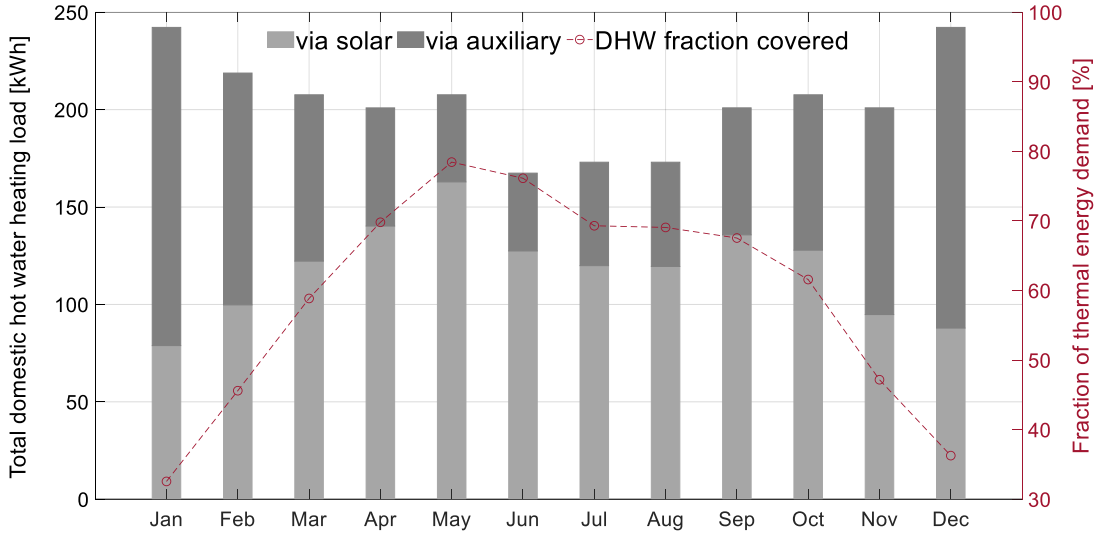

Figure 15 - Monthly fraction of thermal energy demand covered for domestic hot water [10].

Effective heat storage solution is vital for enhancing system performance and economic viability. They significantly improve efficiency, reduce energy wastage, and ensure a reliable, continuous energy supply. Seasonal storage solutions like low-temperature ATES store excess summer heat for winter heating and reserve cold for summer cooling, providing a sustainable climate control solution.

5.3.5. Aquifer thermal energy storage

The seasonal storage system comprises two aquifers: warm (25 ^{o}C) and cold (15 ^{o}C). To meet hourly energy demands (space heating and DHW), water from the warm aquifer is supplied to the heat pump to raise it to the needed temperature (space heating: 35 ^{o}C, DHW: 60 ^{o}C). For space cooling, water from the cold aquifer is used via a heat exchanger. In seasonal storage modeling, a key parameter of interest is the heat balance between the energy extracted and injected into the storage system. Every hour of the year, the temperature and volume of each aquifer are calculated, considering the extraction and injection processes for that period, ensuring optimal performance and sustainability. The thermal balance ensures that the energy extracted from the warm aquifer is equal to the energy stored in the cold aquifer, allowing efficient seasonal energy exchange. Simultaneously, the mass balance maintains

equal volumes of water extracted and injected between the cold and warm aquifers, preserving hydraulic equilibrium.

5.4. Integration of components

5.4.1. System inputs

First, to accurately consider climate conditions, *Meteonorm* is used to get precise weather data for a typical year at a specific location that in this case is Amsterdam city. This involves gathering information on solar irradiation level, ambient temperature, and wind speed, which highly affect how well solar modules work and how much heat a home need. Additionally, building heating and cooling inputs, along with building insulation, are essential factors. The real heating and cooling data are utilized, where heating data includes both space heating and DHW. The available space heating data covers scenarios with the building's current insulation and with new insulation. Effective insulation reduces the energy required for heating and cooling by minimizing heat transfer through the building envelope, ensuring that heating and cooling systems operate efficiently and influencing the overall energy consumption and comfort levels within the building.

5.4.2. Integrated system description

The integration of solar collectors, heat pump, and ATES system forms a highly efficient and sustainable solution for heating and cooling buildings as depicted in Figure 16. The solar collector harnesses solar energy, producing electricity and heat. The thermal energy can then be utilized by the heat pump to meet the heating demands of the building. The ATES system, on the other hand, provides seasonal storage by storing excess thermal energy in underground

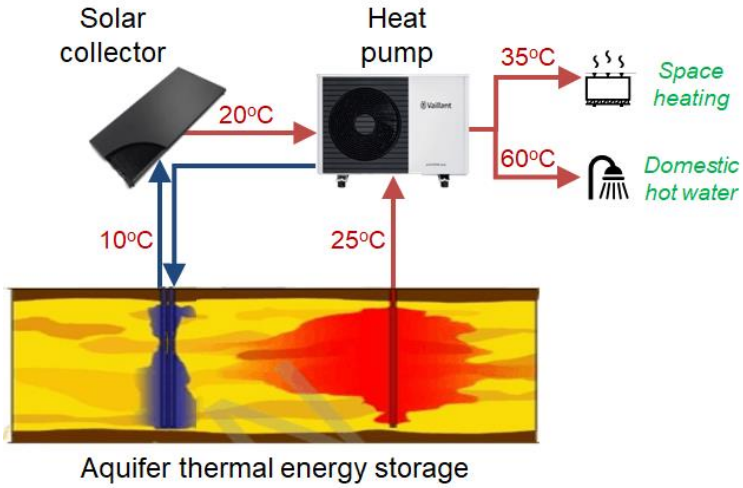

Figure 16 - Solar heating system integrated with solar collectors, heat pump and seasonal storage.

aquifers during periods of low-demand and retrieving it during high-demand periods, such as winter. The ATES system stores surplus heat collected during sunny periods and supplies it back to the system during colder months, ensuring a continuous and efficient energy supply. The separation of the heat pump for solar collectors and ATES systems is critical, as it allows

each system to operate optimally within its specific conditions and timeframes. The solar collectors require its heat pump to function year-round, while the ATES system typically operates during high heat demand periods, such as winter. This separation ensures each heat pump can run at its nominal power, enhancing overall system efficiency and reliability.

5.4.3. Modes of the system

The operational modes of this integrated system are designed to fulfill the heat demand for the building throughout the year in Amsterdam or other focus district, accounting for the weather-dependent nature of solar energy. As illustrated above, the system integrates solar collectors as an energy source along with seasonal storage and heat pump. The heat collected from the solar collector should meet DHW and space heating requirements of each building, maintaining the necessary temperature levels for each application. This process may or may not involve the use of all components, depending on the specific mode.

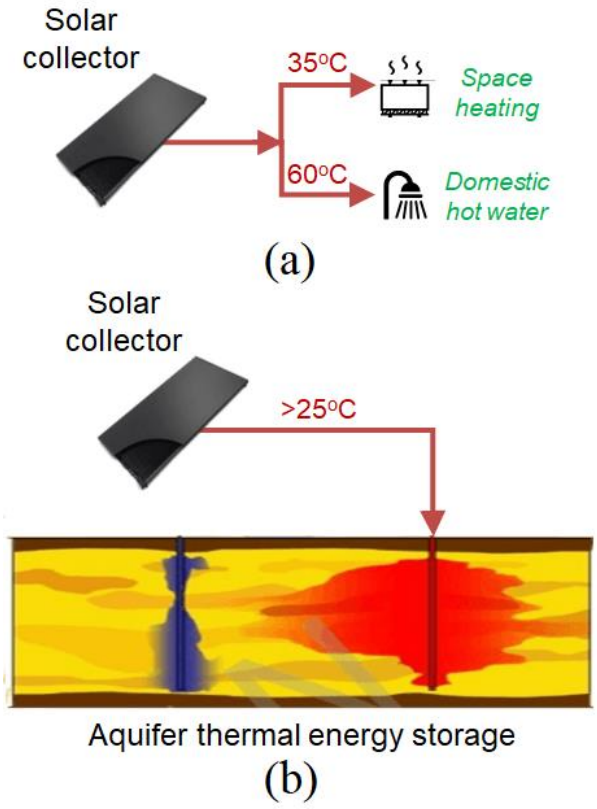

Figure 17 - Operational mode 1 (a) Heat production directly from solar collectors for heating and (b) Excess heat generated by solar collectors is stored directly in the warm aquifer.

To accurately model this system, an energy balance throughout the year must be conducted by considering multiple operational modes that describe the interactions of heat production. The first mode describes the primary heat production during the summer months. In this mode, heat is directly supplied for DHW and/or space heating without using a heat pump, as shown in Figure 17a. When the heat demand is fulfilled or not needed, any residual heat is stored in the warm aquifer of the ATES system, as illustrated in Figure 17b.

Figure 18 illustrates the space heating demand for an 80 m² house, depicted in blue, alongside the heat production by a single PVT system of approximately 2 m², shown in orange. The figure highlights that PVTs predominantly generate heat during the summer months (in purple), whereas the heating demand is highest during the winter months (in red). This indicates that mode 1 covers a very limited amount of heating and seasonal energy storage is required.

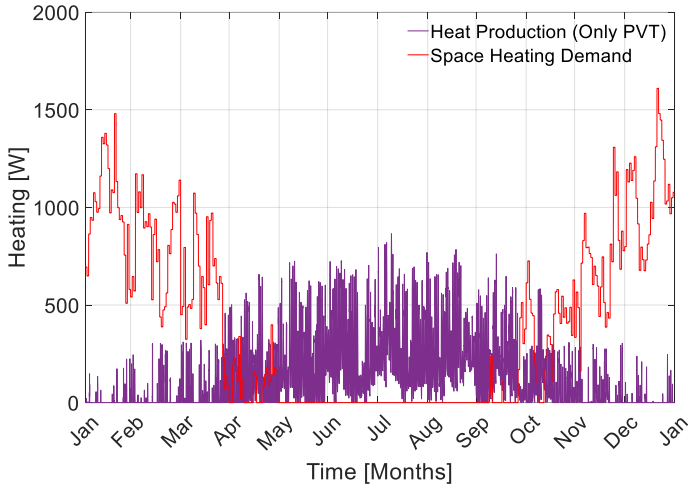

Figure 18 - Heat production of a PVT collector of approximately 2 m² and space heating demand for 80 m² house.

The second mode operates most of the year when the output temperature of the solar collector system is lower than required for DHW or space heating. Here, a heat pump is needed to achieve a sufficiently high temperature for heating as depicted in Figure 19. This mode is primarily used during spring and autumn when the heat demand inside the buildings is moderate.

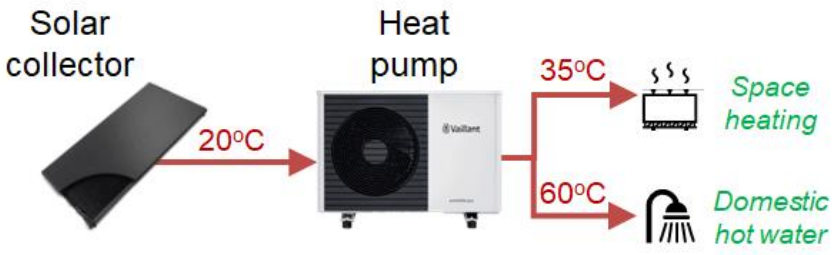

Figure 19 - Operational mode 2, heat produced by solar collectors and enhanced by the heat pump for heating.

In Figure 20, a heat pump is integrated with a single PVT collector, and the results are displayed only for the winter months when heating is needed. It is observed that a PVT combined with a HP can supply a portion of the required heat (in light purple) during winter. By adding additional modules, it is possible to meet the heating demand entirely. However, to minimize the number of solar collectors needed, given the limited roof space, seasonal storage is essential.

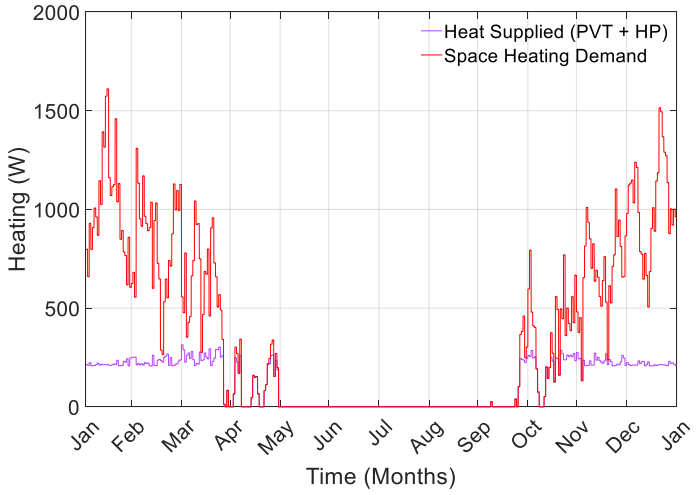

Figure 20 - Heat production of a PVT collector of approximately 2 m² combined with HP and space heating demand for 80 m² house.

The third mode is employed when the heat demand cannot be fulfilled by previous modes. This mode relies on the heat stored in the warm aquifer of the ATES system to meet the households heat demands during the winter. Mode 3, presented in Figure 21, additionally involves a heat pump to enhance the temperature. It is important to store surplus heat during the summer, to ensure adequate heating during the winter months.

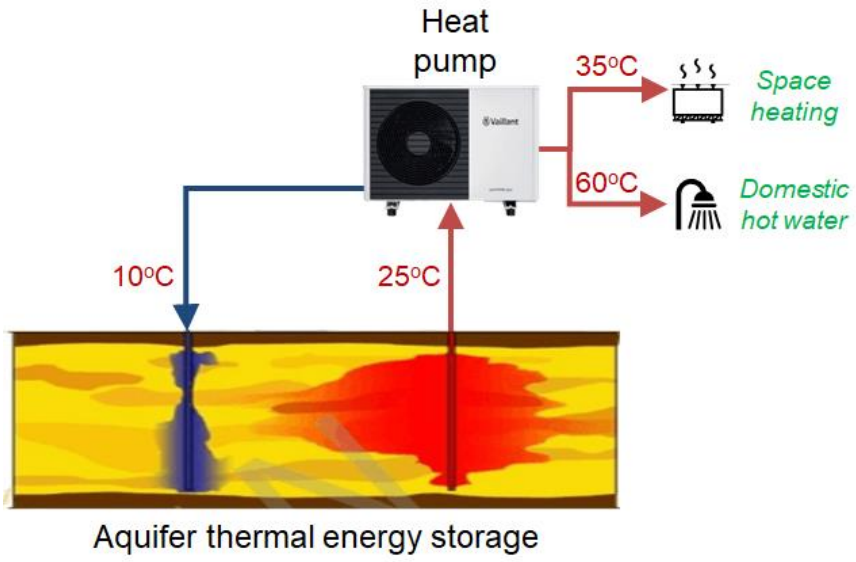

Figure 21 - Operational mode 3, heat extracted from seasonal storage and enhanced by heat pump for heating.

The use of seasonal storage is necessary to fulfill the buildings heat demand, as illustrated in Figure 22. The overall contribution of this mode is crucial for sizing the solar collector system. This is because the heat provided by this mode is produced by solar collectors and stored for winter, ensuring a net-zero balance.

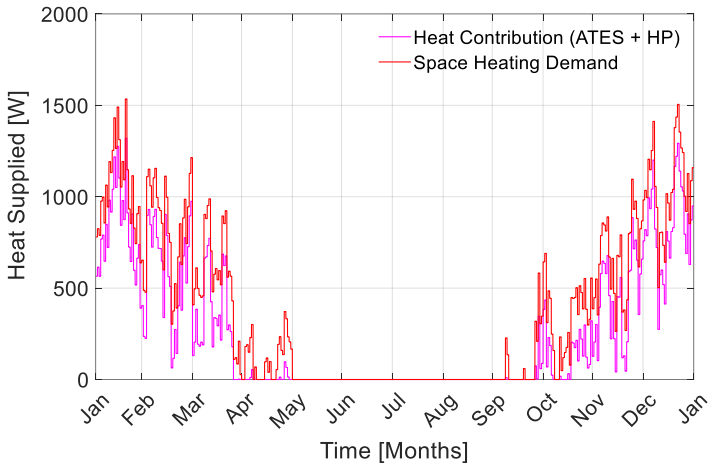

Figure 22 - Heat supplied through ATES and heat pump using a PVT collector of approximately 2 m² for 80 m² house.

Additionally, there is a cooling mode in which the cold aquifer cools the building by exchanging its cold water with the buildings warm water through a heat exchanger. The heat exchanger then sends the warm water back to the warm aquifer and circulates the cold water to the building, effectively meeting the cooling demand. In this example, the modeled system meets 100% of the cooling demand (4.8 MWh) as illustrated in Figure 23 using a cold aquifer which has a volume of 20,000 m³, with a thermal radius of 18.27 m and a hydraulic radius of 27.68 m. The cold aquifer starts the year at 15 ºC and ends at 15.63 ºC.

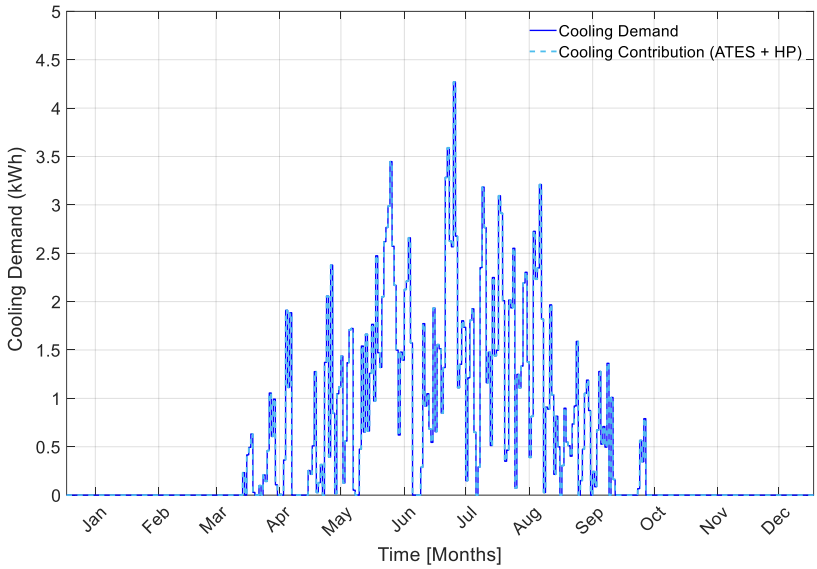

Figure 23 - Cooling through ATES and heat pump for 80 m² house.

5.5. Energetic Output Analysis

5.5.1. Heating and cooling demand

In Amsterdam, the energetic output of solar systems, plays a crucial role in meeting the heating and cooling demands. The heating demand is divided into space heating, which is required mostly during winter and influenced by building insulation, and DHW, needed throughout the year. Traditionally, the city relies on natural gas for heating, but there is a growing shift towards renewable energy sources. Cooling needs are comparatively lower but are rising due to urbanization and climate change, highlighting the importance of integrating energy-efficient building designs and advanced technologies like solar heating/cooling system for sustainable energy management.

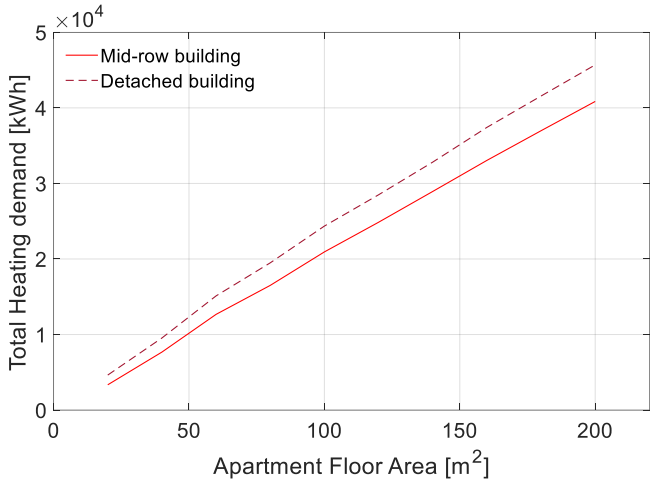

Figure 24 - Annual space heating demand comparison for a four-story building in the Netherlands, considering an average inside temperature of 20 °C.

Floor area is an important parameter, the impact of floor area on heating demand for both four-story mid-row building and four-story detached building, is presented in Figure 24. The heating demand shows a linear relationship. As the floor area increases, the total annual heating demand rises proportionately in both building types. However, detached building experience higher heating demand compared to mid-row building due to their larger exposed surface area, which results in greater heat loss to the environment.

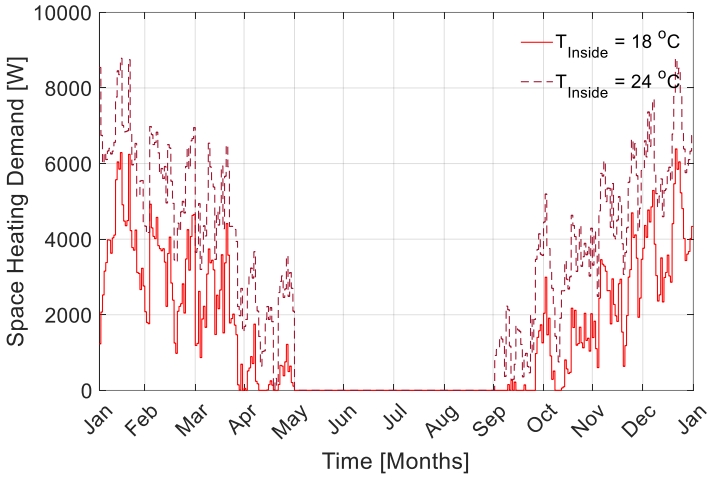

Figure 25 – A comparison of annual space heating demand by setting two different inside temperatures.

The desired indoor temperature significantly impacts heating demand as depicted in Figure 25. High-energy consumers, who prefer an indoor temperature of 24 °C, compared to low-energy consumers, who prefer 18 °C, exhibit almost double the overall heating demand due to the 6 °C difference.

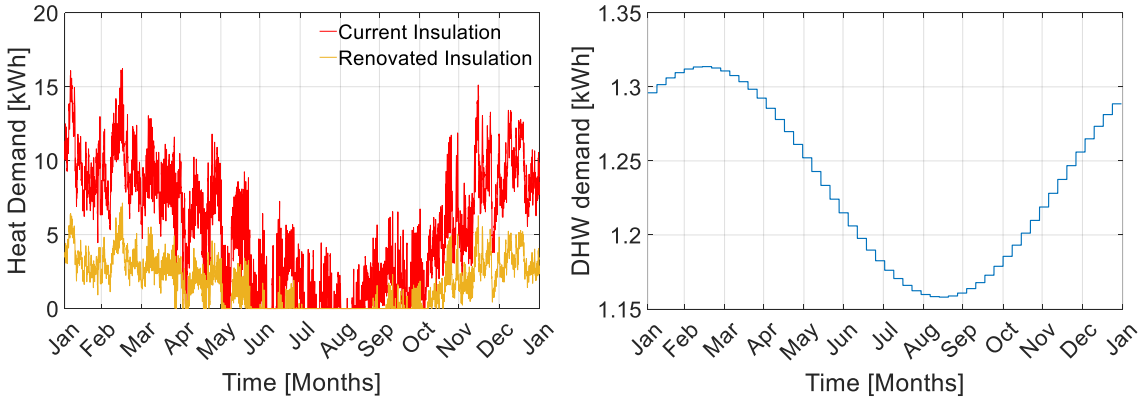

Figure 26 – Space heating demand with current and new insulation (left) as well as DHW load (right) throughout the year for Beursstraat 25.

Effective insulation plays a pivotal role in mitigating heating demands in buildings. Well-insulated buildings require significantly less heating compared to poorly insulated ones, as insulation minimizes heat loss and is shown in Figure 26, a real example of a four-story building in the center of Amsterdam, located at Beursstraat 25. Built in 1700, the building has a roof area of 142 m². With the current insulation, the total space heating demand is approximately 61,500 kWh. However, with improved insulation, the space heating demand can be reduced to approximately 18,700 kWh. However, insulation does not affect the demand for DHW, which is needed year-round and remains the same at about 10,800 kWh. In contrast, space heating is primarily required during the winter months, making insulation particularly important for managing seasonal heating needs effectively.

5.5.2. Analysis of electrical and thermal output data

Two different examples were compared and considered, glazed and unglazed air-based PVT collectors. For a PVT collector, cell temperature and fluid outlet temperature are important. Cell temperature directly affects electrical performance, while fluid outlet temperature impacts the thermal output of the collector. Figure 27 shows the hourly evolution of ambient temperature (in black) and solar irradiance (in blue) over three days in Amsterdam. The maximum solar radiation observed on the first day is just above 800 W/m^2, with the ambient temperature peaking at 25.30 ^{o}C around solar noon. Both configurations used similar wind speed and mass flow rate profiles, with the air inlet temperature assumed equal to the ambient temperature. Over three days, PV module component temperatures peaked, with the glazed configuration (solid line) providing higher thermal output. However, the PV cell temperature in the glazed setup reached around 60 ^{o}C, compared to 46.80 ^{o}C for the unglazed configuration (dashed line), leading to decreased PV performance and lower electrical yield. Similar temperature evolutions can be obtained for the remaining part of the year, not only for cell and fluid components but also for the remaining components of the modules. These results are then used to calculate the annual thermal and electrical outputs of the collectors, with the final aim of obtaining the avoided primary energy (APE).

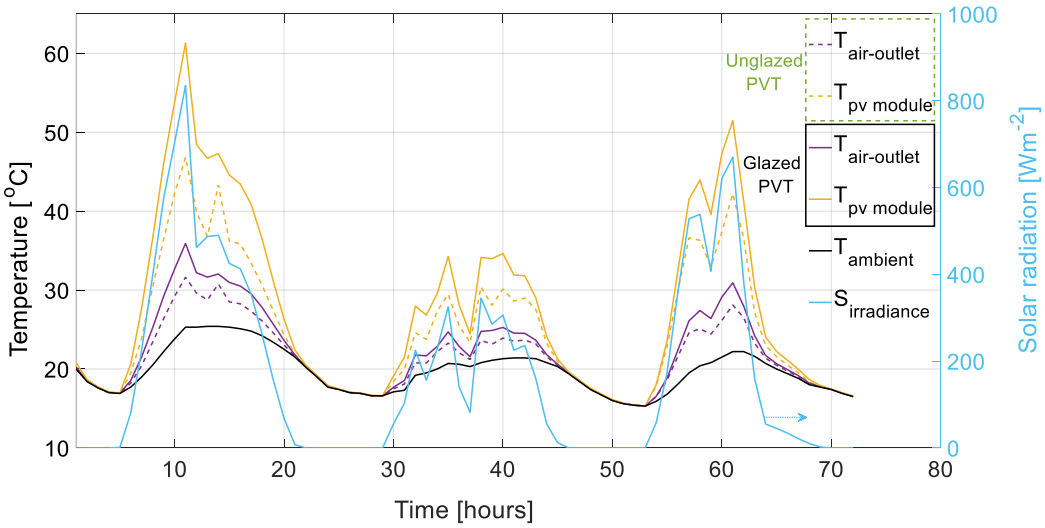

Figure 27 - The hourly evolution of temperature components in glazed and unglazed air-based PVT collector in Amsterdam region.

5.5.3. Energy yield calculations

To determine the thermal and electrical yield of the solar collector, the component temperatures were used. The monthly solar radiation profile in Figure 28 (bottom left) for the Amsterdam region shows solar energy availability throughout the year. Solar radiation peaks in the summer and dips in the winter. The average monthly ambient temperature profile (in solid black line) highlights typical annual temperature variations, with the coldest temperatures in January and December and the warmest in July. The seasonal cycle is clearly

visible in this temperature data. The figure also compares monthly electrical and thermal energy production for two PVT configurations (top-right - unglazed and top-left - glazed).

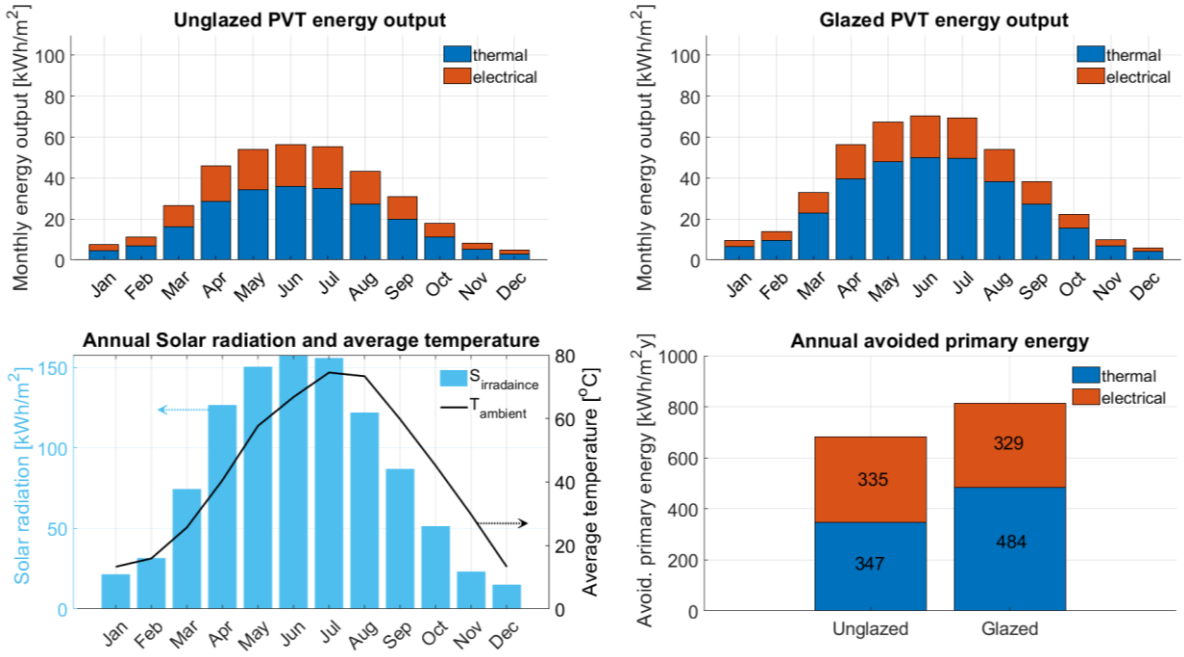

Figure 28 - Monthly prediction of thermal and electrical energy outputs, bottom right - avoided primary energy (APE) per m² for glazed and unglazed air-based collectors and bottom left - monthly solar radiation and average ambient temperature in Amsterdam region.

Energy production is lower in the winter and peaks in May, June, and July due to high solar irradiation and abundant sun hours. The glazed configuration produces the highest annual thermal output but the lowest annual electrical output (approximately 131 kWh/m^2). In the bottom-right of the figure, a comparison of APE per square meter which is explained above shows approximately 682 kWh/m^2 per year for the unglazed configuration and around 813 kWh/m^2 per year for the glazed configuration.

5.5.4. Comparison of PVT with traditional PV and ST modules

PVT collectors combine the benefits of both solar electricity and heating in one unit, making them ideal for situations needing both types of energy. However, they can be more expensive and complex. Traditional PV and ST modules on the other hand have their own strengths and are better suited for specific needs, so the best choice depends on what energy requirements. Figure 29 shows the temperature difference between the fluid outlets of the PVT collector and ST module. The ST module outlet temperature is higher than that of the PVT module throughout the year, indicating that the ST module is better at producing heat. Specifically, the ST module consistently achieves higher temperature increases than the PVT module whenever there is any irradiation during the day. However, the PVT collector also generates electricity, while the ST module only produces heat.

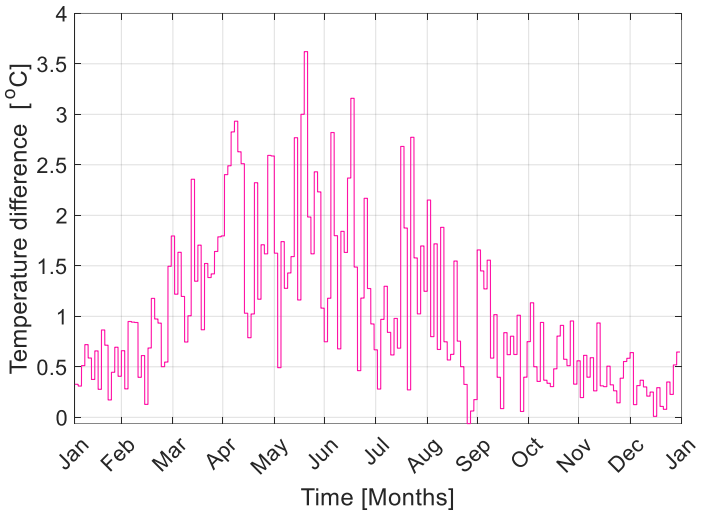

Figure 29 – Water outlet temperature difference while comparing the thermal output behavior of a PVT module and a ST module.

Next, we explore the suitability and optimal combinations of different solar collectors. In the presented Figure 30, it is evident that as the apartment area increases, fewer PVT modules are required to cover the heat demand compared to using ST collectors combined with PV modules. This is because heat pump requires substantial power for heating, and PV modules can effectively supply this power. Meanwhile, PVTs provide both heating and electricity from same unit, making them a better solution in terms of performance and energy calculations.

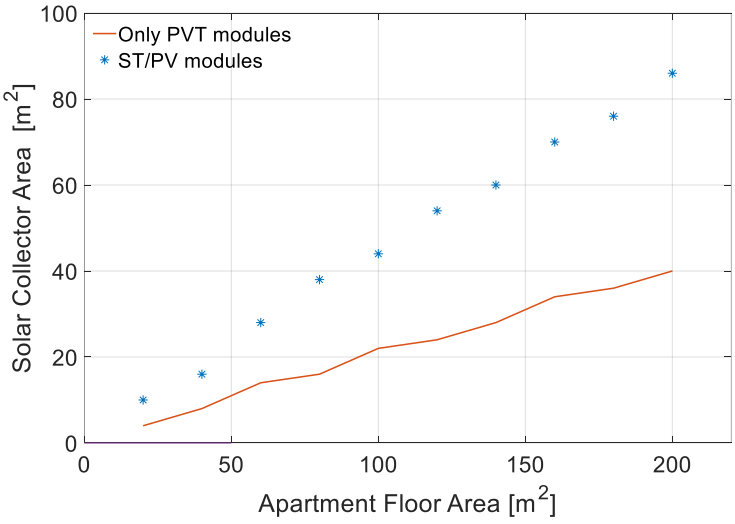

Figure 30 - Required solar collectors for various house areas using various solar collector types.

In summary, PVT collectors may exhibit lower individual efficiencies in generating electricity and heat compared to their separate PV and ST counterparts, their ability to simultaneously produce both forms of energy results in a higher overall energy yield per square meter. The APE metric as presented in Figure 11, considering the efficiencies of conventional energy conversion methods, offers a comprehensive measure of this enhanced performance.

5.5.5. Economics and environmental impact

The annual comparison of the levelized cost of electricity (LCOE) and CO_2 mitigation for glazed and unglazed air-based PVT collectors is presented in Figure 31. The data shows that glazed

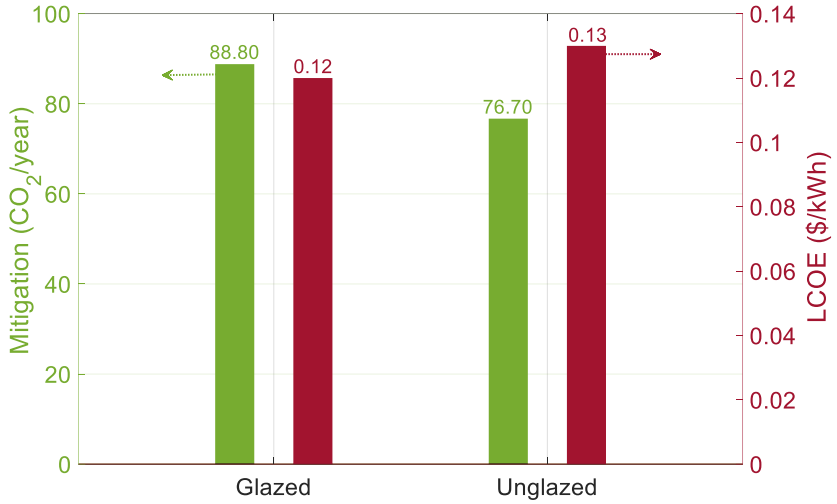

Figure 31 - Annual comparison of levelized cost of electricity (LCOE) and CO_2 mitigation for glazed and unglazed air-based PVT collectors.

collectors exhibit superior performance in both economic and environmental metrics. Specifically, glazed collectors avoid annual emissions at a minimum of 88.80 $kgCO_2$, outperforming the unglazed collectors with 76.70 $kgCO_2$/year. The LCOE for glazed collectors is 0.12 $/kWh, compared to the higher LCOE of 0.13 $/kWh of their unglazed counterparts. This shows the efficiency and cost-effectiveness of glazed PVT collectors, making them a more attractive option for sustainable energy solutions.

Additionally, the economic analysis of an integrated system with various components, including solar collectors, seasonal storage, heat pumps, heat exchangers and submersible pumps, is thoroughly examined for the buildings Beursstraat 5, 21, Oudebrugsteeg 3, and Warmoesstraat 96 located in the city center of Amsterdam. The study focuses on the financial viability of the system compared to traditional heating and cooling methods. The analysis considers several costs, such as capital, operational, and replacement expenses [13-15]. Capital costs encompass one-time expenditures like site investigation, drilling, and installation of pipes, valves, and meters to manage water flow and the costs are provided in Table 2. Operational costs are estimated to be 4% of the capital costs [16], totaling €295,000 over the systems 25-year lifespan [17-20]. The systems energy demand is substantial, requiring approximately 70 MWh to power the heat pumps and submersible pumps. To meet this demand, 190 PV modules and 10 PVT collectors are required, generating around 365 kWh each from approximately 2 m^2 area.

Table 2 - Capital cost breakdown of the integrated system main components.

Category	Cost (€)
Pre-investigation and preparation	9600
Well piping and insulation	27,600
Building integration	44,250
Solar collectors	61,800
Piping	139, 200
Controlling and monitoring	6000
Drilling	6500

The study calculates an annual interest payment of €14,750 based on the capital costs. The ATES system delivers a yearly thermal energy output of 298,400 kWh. By dividing the total annual costs mentioned in Table 3 by this output, the levelized cost of thermal energy is determined to be approximately €0.13/kWh. This comprehensive analysis provides valuable insights into the economic feasibility of the system, highlighting its potential as a cost-effective alternative to conventional methods.

Table 3 - Integrated system cost breakdown.

Category	Cost (€)
Annual depreciation	11,800
Annual operational costs	11,800
Annual replacement costs	75
Annual interest payment	14,750
Total annual costs	38,425

A detailed analysis of the carbon emissions reduction achieved by the integrated system when compared to conventional gas-based energy sources is also presented. The analysis evaluates emissions from gas-based sources used for space heating, cooling, and DHW demands. The integrated system utilizes solar collectors to power heat pumps and submersible pumps, offering an environmentally friendly alternative to traditional grid electricity, which relies on a mix of fossil fuels and renewable energy. Key to this analysis are the emission factors, which provide the CO_2 emissions per unit of energy consumed.

Specifically, fossil-fuel-based electricity has an emission factor of 617 kg CO_2/MWh, while gas has an emission factor of 277 kg CO_2/MWh [21]. These factors are essential for calculating the environmental impact of energy consumption in both conventional and integrated systems. The work highlights the significant emissions reductions achieved by the integrated system compared to a gas-powered district heating system. The system achieves annual reductions of approximately 55 tonnes of CO_2 for space heating, 5 tonnes for space cooling, and 23 tonnes for DHW. Over the 25-year lifespan of the system, these reductions amount to a total of 2,075

tonnes of CO_2. This substantial reduction underscores the environmental benefits of the integrated system, making it a compelling alternative to traditional gas-based methods. By significantly lowering carbon emissions, the integrated system not only provides financial advantages but also contributes to a more sustainable future.

5.6. Focus District of Amsterdam

This section provides an analysis of solar energy potential within a specific district of Amsterdam. The focus is on determining the number and type of solar collectors necessary to meet the energy demands of multiple buildings within the district. Additionally, it compares the effectiveness and energy yield of solar collectors in different regions of Amsterdam.

5.6.1. Solar collectors required to cover demand for multiple buildings

First, consider real examples of 3 to 5-story buildings in the center of Amsterdam, specifically located at Beursstraat 5, 21, 25, Oudebrugsteeg 3, and Warmoesstraat 96. Built around 1700, these buildings have roof areas ranging from 69 to 163 m², as depicted by the yellow bars in Figure 32. With the current insulation, the total space heating demand is high (Beursstraat 21 - 43,700 kWh, Beursstraat 25 - 61,600 kWh, Beursstraat 5 – 49,400 kWh, Oudebrugsteeg 3 – 31,300 kWh and Warmoesstraat 96 – 19,900 kWh). However, improving the insulation can significantly reduce the space heating demand as shown in the figure. The DHW demand remains unchanged and is unaffected by insulation improvements. Among these buildings, Beursstraat 5 has a much higher demand despite its low surface area. In contrast, Warmoesstraat 96, which has a larger available roof area, exhibits a lower heating demand.

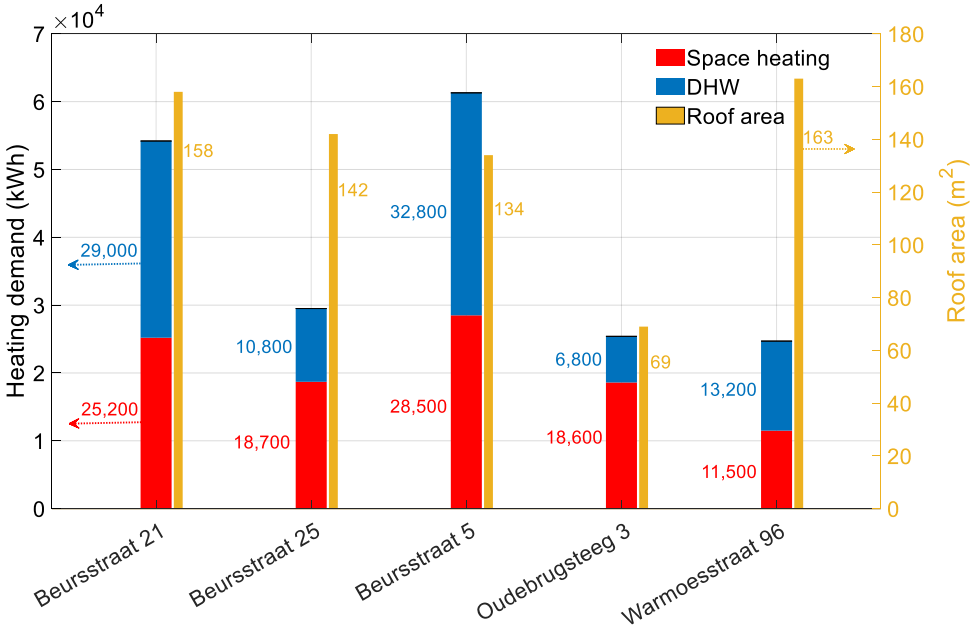

Figure 32 - Annual heating demand with current insulation and roof are of multiple buildings in Amsterdam.

The number of solar collectors required to cover the space heating demand, comparing current and new insulation across multiple buildings in Amsterdam, as well as for DHW is

presented in Figure 33. It can be observed that significantly fewer PVT collectors are needed for heating compared to the combination of PV and ST modules. PVT collectors are advantageous because they generate both heat and electricity from the same surface area, highlighting their benefits over conventional ST and PV modules. Additionally, with improved insulation, the number of required modules decreases substantially. However, the number of modules required for DHW remains same with the renovation. The highest number of modules is needed for Beursstraat 5, which has the highest demand.

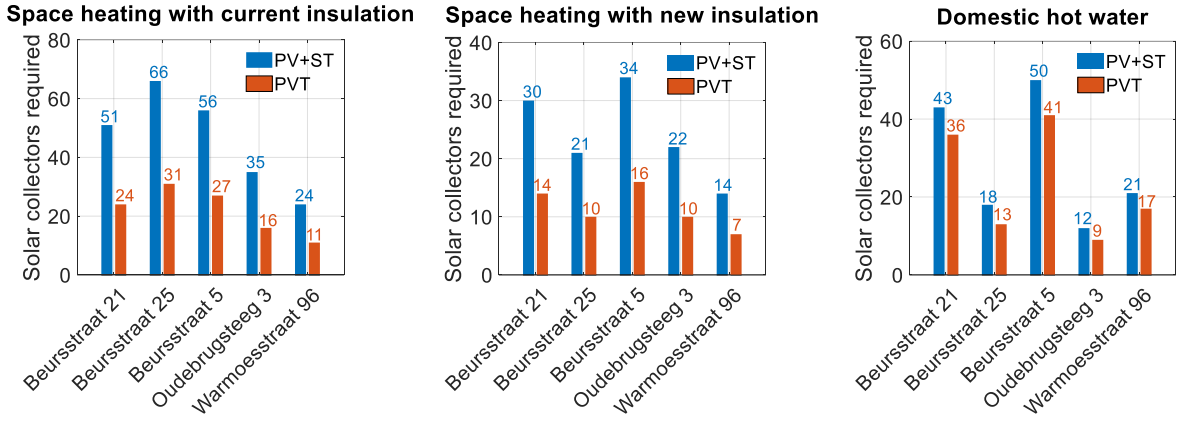

Figure 33 - Number of solar collectors required to cover heating demand, comparing current and new insulation across multiple buildings in Amsterdam.

For the buildings taken into consideration, with the current insulation, Mode 1 (only solar collectors) contributes between 4.10% and 7.30%, Mode 2 (with a heat pump) contributes

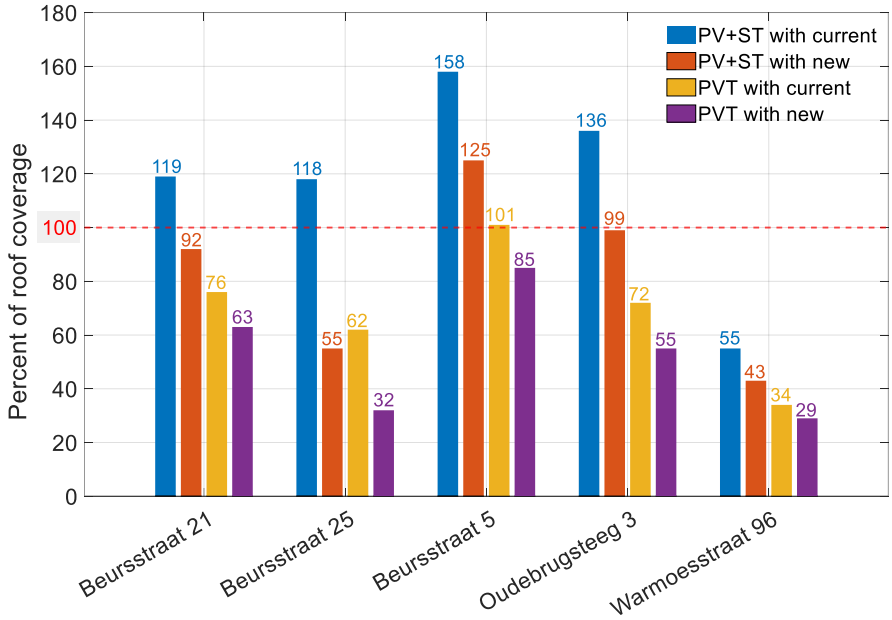

Figure 34 - Percentage of roof coverage with various solar collector types, comparing current and new insulation across multiple buildings in Amsterdam.

between 66.40% and 69.40%, and Mode 3 (with seasonal storage) contributes between 23.30% and 29.50%. However, with improved insulation, the percentages for Mode 1 decrease

to between 2.60% and 4.20%, while Mode 2 remains approximately the same, between 66% and 67.70%. In contrast, the contribution of Mode 3 increases to between 29.80% and 31.40%.

The percentage of roof coverage with various solar collector types, comparing current and new insulation across multiple buildings in Amsterdam is shown in the above Figure 34. Two different combinations of solar collectors were analyzed: PVT and a combination of PV and ST modules. The results, considering both space heating and DHW, indicate that for Warmoesstraat 96, the roof area required is always below 100% as the available roof area is 163 m^2, much higher than the rest. However, for other buildings with current insulation, the combined PV and ST modules are not feasible due to exceeding available roof space. New insulation improves the situation, reducing the required roof area, but PVTs require substantially less space compared to the separate use of PV and ST modules. This suggests that for buildings with limited roof area, employing PVTs exclusively is more effective in meeting energy demand.

5.6.2. A comparison between solar collectors yield across multiple regions in Amsterdam

A new tool has been developed in python language to primarily handle a wider variety of input data formats and allow for the more advanced calculations. In this example the solar irradiation for the solar modules on the building groups in the Focus District of the center of

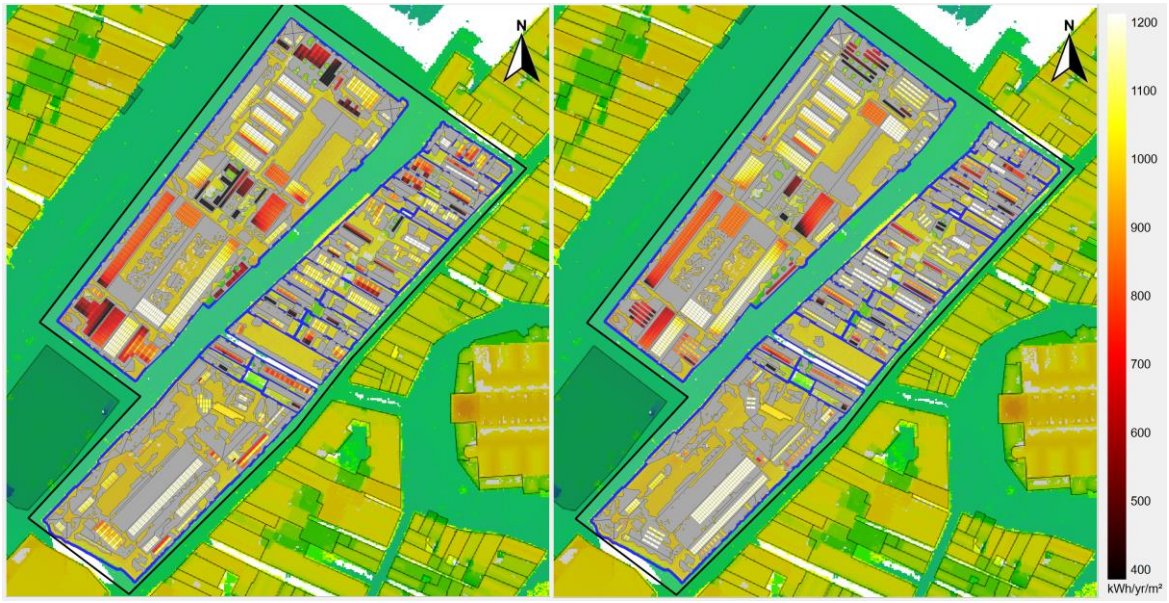

Figure 35 - Solar irradiation for solar modules for building groups in the focus district of the center of Amsterdam with east west-landscape (left) and south facing-portrait (right).

Amsterdam is shown in Figure 35 with layout and orientation. The images show (left) a combination of east-west facing layout for zero-tilt surfaces and landscape orientation for sloped surfaces and (right) south-facing layout for zero-tilt and portrait orientation for sloped surfaces. The grey shapes show the detected suitable roof surfaces for modules. The detected surfaces do not cover all the rooftop, due to the more complex roof structures in the city center.

Using the hourly irradiance and meteorological data, we can calculate the electrical yield of PVs, thermal yield of glazed STs and the electrical and thermal energy yield of unglazed PVTs for every module. The results are shown in Figure 36 for the city center and AMS institute. The results are for south-facing and portrait combined and it can be observed that PVTs performance is much better per m^2 as compared to the combined use of standalone PV and conventional ST module. Not only per m^2, also the electrical output for PVTs is higher due to the use of heat extraction medium. The use of glazing on top of the ST module increases the thermal output but in case of PVT. If glazing is used, the electrical efficiency decreases, which results in lower PVT electrical output.

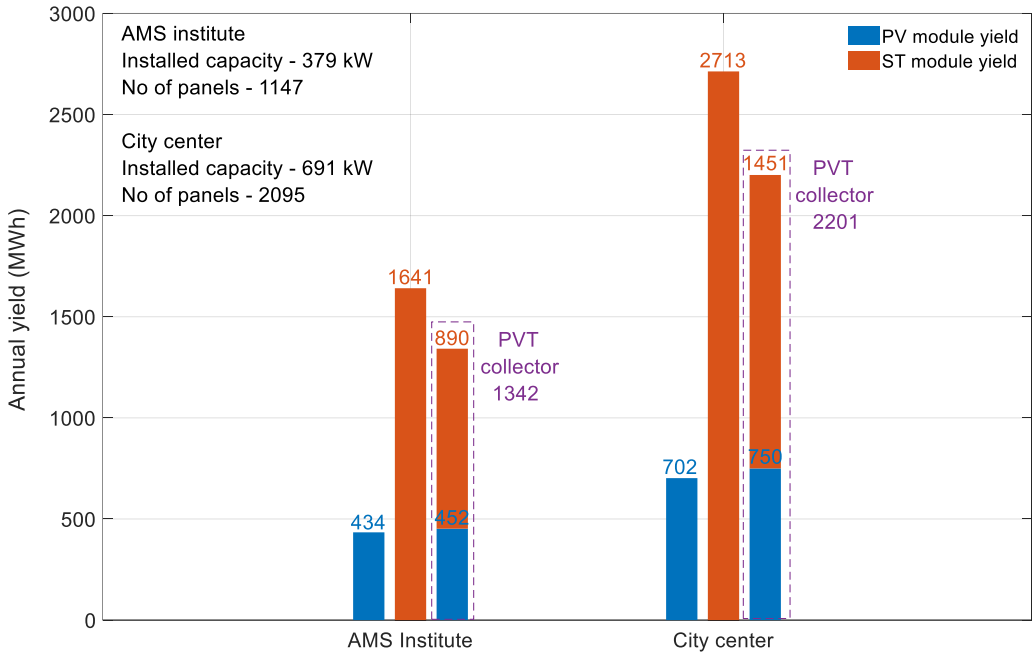

Figure 36 - Solar collectors electrical and thermal yield for multiple locations.

Using the hourly irradiance and meteorological data, we calculated the electrical and thermal yield of various PVT collectors based on flow passages [22] across the entire city center of Amsterdam. The area considered for the air-based PVT collector is 0.5 m^2, for the serpentine tube PVT it is 1.63 m^2, while for the remaining PVT configurations, it is approximately 2 m^2. Figure 37 shows that the module count for the air-based PVT is 1,739,234, for the serpentine tube PVT it is 473,812, and for the other configurations, it stands at 385,397. The installed capacity for each PVT configuration is also displayed in this figure. From this data, it is evident that the air-based PVTs, due to their smaller area, result in significantly higher module numbers, though the larger area required for the serpentine tube and other configurations limits their module count. Due to the small size of the modules, solar irradiation on the buildings in the city center is not presented. However, the number of PVT modules (Serpentine tube configuration) as an indication for how the PVTs are distributed in the city center is shown on the cover page of this report.

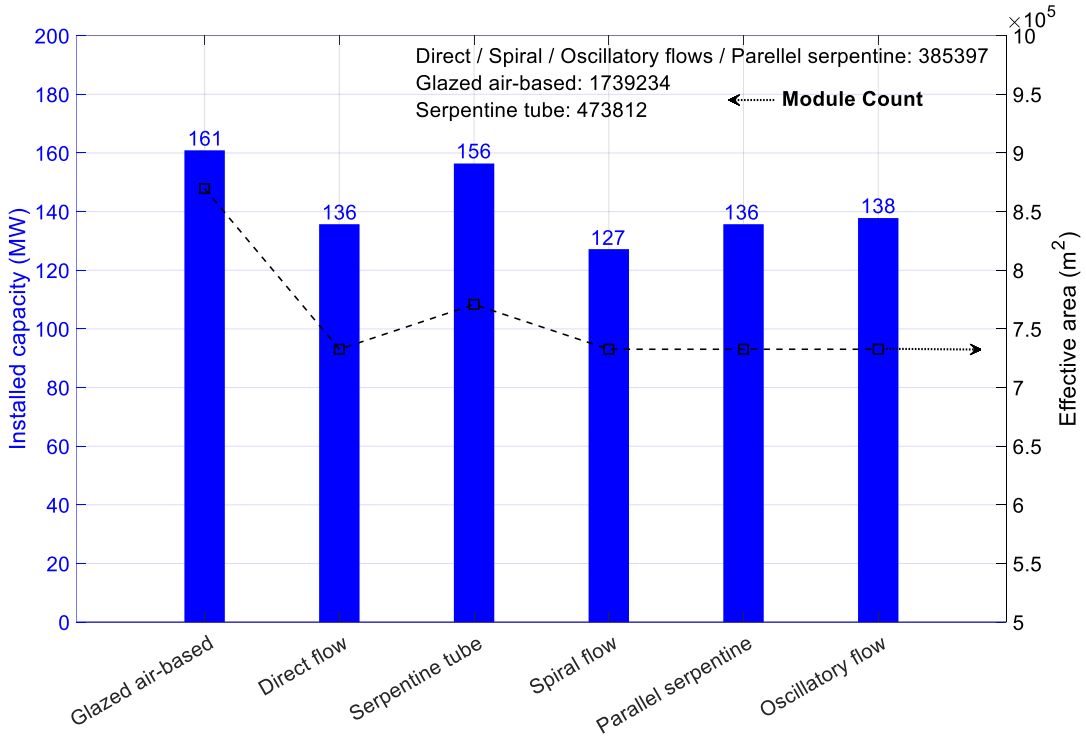

Figure 37 - Installed capacity, effective area and PVTs module count for the whole center of Amsterdam.

Figure 38 shows that the air-based PVT collector has the lowest overall performance, approximately 495 kWh/m², compared to the water-based collectors. The serpentine tube

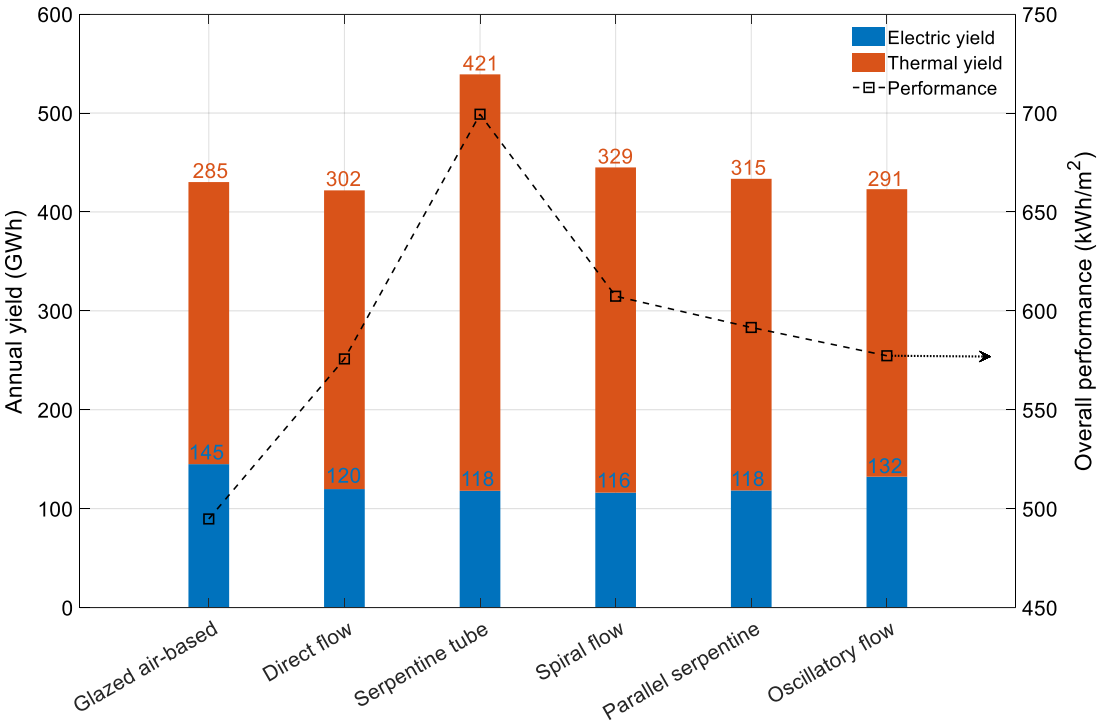

Figure 38 - Solar PVT collectors electrical and thermal yield for the whole center of Amsterdam.

PVT achieves the highest performance at 700 kWh/m², while the other PVTs with various flow passages perform between 570 and 620 kWh/m². Despite its lower performance, the air-based PVT has a higher electrical annual yield due to its smaller collector area. The serpentine tube PVT delivers the highest total annual yield, around 540 GWh, while other PVT configurations range from 422 to 445 GWh. The serpentine tube configuration higher yield can be attributed to its slightly smaller collector area and more number of modules that can be accommodated on the roofs. Considering Dutch climate where solar radiation is not that high, the heat extraction medium flows for a shorter duration in serpentine tube configuration and efficiently captures enough heat from the top, whereas other configurations have larger module areas and captures the same amount of heat which results in lower thermal yield.

Conclusions

In conclusion, a geo-referenced multi-layer mapping of Amsterdam district provide a detailed assessment of solar potential by overlaying several factors. This document provides an overview of PV systems and PVT systems integrated with seasonal storage and heat pump. It further includes a report on the energy yield potential of PVT modules for the city center of Amsterdam. The main findings of this report are summarized as follow:

- East-west layout yields more energy due to more panels, while the south-facing orientation performs better but with fewer panels. Landscape orientation allows efficient placement, and portrait orientation offers better positioning.
- The simulation approach ensures PV module visibility compliance with municipal guidelines by analyzing pedestrian viewpoints, sightlines, and obstructions.
- When it comes to APE, a PVT collector shows the biggest energy savings per m2 (≈ 973 $kWhm^2$ per year), liquid-based ST module (≈ 877 $kWhm^2$ per year) while PV only module exhibits the smallest (≈ 404 $kWhm^2$ per year) in Amsterdam region.
- Small heat storage tanks work well for short-term energy needs, but seasonal storage provides long-term sustainability and efficiency for urban energy systems.
- Integrating seasonal storage and heat pumps with solar collectors enhances energy output and reliability. However, the combination of seasonal storage and heat pumps meets most of the heat demand in various system modes.
- PVT systems efficiently produce both heat and electricity in less space than conventional PV and solar thermal modules, making them ideal for buildings with limited roof areas.
- A good thermal insulation helps reduce the need for heating. This means fewer modules are needed and less roof space is used.
- A small economic analysis was conducted for the integrated system, revealing that the levelized cost of thermal energy is approximately €0.13 per kWh. Additionally, over the 25-year lifespan of the system, the implementation of this integrated approach leads to a substantial reduction in carbon emissions.
- We analyzed five old buildings in the city center and found them to be energy positive. However, analyzing the entire city center is not possible, considering the complexity of solar collectors integrated with ATES and heat pump.
- Simulations revealed that the serpentine tube PVT configuration outperformed air-based and other liquid-based systems in annual energy yield across the entire city center.

Sources

[1] Assessing Roof Suitability for Solar Panel Installation, https://www.illuminei.com/blog/assessing-roof-suitability-for-solar-panel-installation

[2] Groene en multifunctionele daken https://maps.amsterdam.nl/open_geodata/?k=51

[3] Beschermde dorps- en stadsgezichten https://maps.amsterdam.nl/open_geodata/?k=125

[4] Historische monumenten https://maps.amsterdam.nl/open_geodata/?k=118

[5] Amsterdam Rainproof bottlenecks https://maps.amsterdam.nl/open_geodata/?k=288

[6] Verkou, Maarten, Zameer Ahmad, Hesan Ziar, Olindo Isabella, and Miro Zeman. "A Multi-layer Modelling Framework for Techno-Socio-Economical Penetration of Photovoltaics." In *2021 IEEE 48th Photovoltaic Specialists Conference (PVSC)*, pp. 1685-1686. IEEE, 2021.

[7] Height data retrieved from algemeen hoogtebestand Nederland, https://www.ahn.nl/open-data

[8] Bag Cadaster data from bag viewer, https://bagviewer.kadaster.nl/lvbag/bag-viewer/

[9] Stalin, P. Michael Joseph, et al. "Performance improvement of solar PV through the thermal management using a nano-PCM." Materials Today: Proceedings 50 (2022): 1553-1558.

[10] Ul-Abdin, Zain, Miro Zeman, Olindo Isabella, and Rudi Santbergen. "Investigating the annual performance of air-based collectors and novel bi-fluid based PV-thermal system." *Solar Energy* 276 (2024): 112687.

[11] Ul-Abdin, Zain, and Ahmed Rachid. "A survey on applications of hybrid PV/T panels." Energies 14, no. 4 (2021): 1205.

[12] Widyolar, Bennett, Lun Jiang, Jordyn Brinkley, Sai Kiran Hota, Jonathan Ferry, Gerardo Diaz, and Roland Winston. "Experimental performance of an ultra-low-cost solar photovoltaic-thermal (PVT) collector using aluminum minichannels and nonimaging optics." *Applied energy* 268 (2020): 114894.

[13] Ingenieurgesellschaft fur Geo-und Umwelttechnik. (2017). Kostenschatzung geothermieanlage. Ingenieurgesellschaft fur Geo- und Umwelttechnik.

[14] Bloomquist, R. Gordon. "Geothermal heat pumps five plus decades of experience in the United States." In *Proceedings World Geothermal Congress 2000*, pp. 3373-3378. 2000.

[15] TripleSolar - The pvt system, https://triplesolar.eu/

[16] Schipper, Simon, Paul Fleuchaus, and Philipp Blum. "Techno-economic and environmental analysis of an Aquifer Thermal Energy Storage (ATES) in Germany." *Geothermal Energy* 7 (2019): 1-24.

[17] Stadtwerke Waldkraiburg. (2018). Preisblatt geothermale fernwarmeversorgung (Report on geothermal district heating pricing). Stadtwerke Waldkraiburg GmbH. Waldkraiburg.

[18] Leistungsbuch altlasten und flachenentwicklung (2015), http://www.leistungsbuch.de/Frontend/%20lbuKatalog/KatalogForm.aspx

[19] Vanhoudt, Desmedt, J. Desmedt, J. Van Bael, N. Robeyn, and H. Hoes. "An aquifer thermal storage system in a Belgian hospital: Long-term experimental evaluation of energy and cost savings." *Energy and Buildings* 43, no. 12 (2011): 3657-3665.

[10] International Energy Agency, Solar Heating and Cooling Programme. (2021). Task 60: Pvt systems, 2021-07-Task60-PVT-Systems.pdf (iea-shc.org)

[21] Energy performance of buildings – Overall energy use and definition of energy ratings, Institute of Petroleum Standard methods for analysis and testing of petroleum and related products, and British Standard 2000 Parts, 2006 (en-standard.eu)

[22] Ul Abdin, Zain. "Modeling and control of hybrid PV thermal panels." PhD diss., Université de Picardie Jules Verne, 2022.

simply positive